This dissertation has been
microfilmed exactly as received 67-3981

QASSEMZADEH, Hassan, 1932-
INVESTIGATION OF THE FAST STRIATIONS IN PRE-BREAKDOWN OF A GAS DISCHARGE USING MICROWAVE RECEIVER TECHNIQUES.

The University of Oklahoma, Ph.D., 1967
Physics, electronics and electricity

University Microfilms, Inc., Ann Arbor, Michigan

Downloaded from SHAREOK. Persistent Handle URL: https://hdl.handle.net/11244/2138

THE UNIVERSITY OF OKLAHOMA

GRADUATE COLLEGE

INVESTIGATION OF THE FAST STRIATIONS IN PREBREAKDOWN OF A GAS DISCHARGE USING MICROWAVE RECEIVER TECHNIQUES

A DISSERTATION

SUBMITTED TO THE GRADUATE FACULTY

in partial fulfillment of the requirements for the

degree of

DOCTOR OF PHILOSOPHY

BY

HASSAN QASSEMZADEH

Norman, Oklahoma

1966

INVESTIGATION OF THE FAST STRIATIONS IN PREBREAKDOWN OF A GAS DISCHARGE USING MICROWAVE RECEIVER TECHNIQUES

APPROVED BY

DISSERTATION COMMITTEE

ACKNOWLEDGEMENT

Dr. James D. Palmer is sincerely acknowledged for directing this dissertation. His constant interest throughout the work has been a major source of encouragement. His suggestions in all stages of the work have been essential in the fulfillment of this investigation.

Gratitude is extended to Dr. Jack Reynolds who, in the course of the experimental work, willingly gave help of material nature and otherwise any time such help was needed.

The special efforts of Mr. Norman Alexandre are appreciated for building the discharge tube.

Finally, much credit goes to my wife for her help, encouragement, and patience throughout this work.

TABLE OF CONTENTS

	Page
LIST OF ILLUSTRATIONS	v
Chapter	
I. INTRODUCTION	1
II. GENERAL CONSIDERATIONS	4
III. THE PRESENT WORK - OBSERVATION OF FAST STRIATIONS	46
IV. RESULTS, CONCLUSIONS, AND RECOMMENDATIONS	59
BIBLIOGRAPHY	76
Appendix	
1. MEASUREMENT OF STRIATION VELOCITY USING MICROWAVE RECEIVER TECHNIQUES	79
2. MICROWAVE REFLECTION FROM A PULSED DISCHARGE	98
3. FURTHER INVESTIGATION OF THE ORIGIN AND GROWTH OF STRIATIONS	114

LIST OF ILLUSTRATIONS

Figure	Description	Page
1	Total discharge voltage and frequency of oscillations as functions of current for a glow discharge	7
2	Voltage and intensity oscillations in the glow discharge	9
3	Oscilloscope pictures of moving striations in argon at constant pressure	10
4	Oscilloscope pictures of moving striations near the cathode in argon at constant pressure and constant current	11
5	Schematic plotting of the wave of stratification . .	20
6	Scheme of two chains of processes which can lead to successive production of striations	23
7	Course of light intensity $i_\nu\theta$ in ν-th region for $\nu = 2,4,8$ as a function of time, t/τ	33
8	Course of sclutions (II-48) to (II-51) for deflection from equilibrium state of concentration of positive ions (n_+) and electric field (e) for five values of t as a function of x	39
9	Time dependence of deflections of concentration of positive ions (n_+) according to (II-50) at two different distances from point of disturbance . . .	40
10	Curves of maxima and minima of deflections of concentration of positive ions (n_+) according to solutions (II-50) as a function of time and distance from disturbance	43
11	Block diagram of the experimental apparatus	52
12	Photograph of the experimental apparatus	53

Figure	Description	Page
13	Simplified sketch of Pekarek's apparatus for perturbation of the cathode end of the positive column	55
14a	Doppler spectrum for a microwave frequency f_0 = 11.122 GHz	61
14b	Doppler spectrum for a microwave frequency f_0 = 11.122 GHz	61
14c	Doppler spectrum for a microwave frequency f_0 = 11.300 GHz	62
14d	Doppler spectrum for a microwave frequency f_0 = 11.300 GHz	62
14e	Doppler spectrum for a microwave frequency f_0 = 11.652 GHz	63
14f	Doppler spectrum for a microwave frequency f_0 = 11.652 GHz	63
15	Method of irradiating the cathode for a uniform electron emission	68
16	Relative sequence of the application of external perturbation	71
17	Method and point of perturbation of the discharge	71
18	Ordinary microwave reflectometer	81
19	Graphical illustration of frequency conversion on the basis of d-c characteristic of crystal	85
20	Typical curve for conversion loss vs. local oscillator drive	87
21	Block diagram for the analysis of the network noise figure	88
22	Conversion loss and noise temperature as a function of rectified current for a typical 1N23B crystal rectifier	96
23	Receiver noise figure as a function of rectified current for a 1N23B rectifier plotted in Fig. 22	96
24	Circuit diagram for the pulsed light source	119

Figure	Description	Page
25	Schematic diagram of pulsed light source. A and B are main electrodes, T is the trigger electrode	120
26	Block diagram-schematic representation of experiments for investigating striations	122

INVESTIGATION OF THE FAST STRIATIONS IN PREBREAKDOWN OF A GAS DISCHARGE USING MICROWAVE RECEIVER TECHNIQUES

CHAPTER I

INTRODUCTION

The existence of moving striations in the positive column of a glow discharge was discovered in 1843 [35]. Since then considerable effort has been made in both methods of observation as well as the theoretical explanation of moving striations [3,4,21,23,32,35]. Some progress has been made in improving methods of observation of a steady state striated glow discharge but up to the present no theory has satisfactorily explained the phenomena leading to striations in a discharge.

In an experimental study made by Donahue and Dieke [3] to observe striations in the positive column of a glow discharge it was found that striations are sometimes stable and repeat themselves for hours but often several modes exist and the discharge moves back and forth between them and appears unstable. Concerning these modes, they find two kinds of oscillations which they call positive and negative striations according to their velocity of motion. They observe more than one negative striation for each positive one. They report, under certain circumstances, as many as nine striations to every two positive ones. In general under a specific condition in the steady-state discharge more than one mode exists giving rise to an unstable, complicated non-reproducible picture.

In an effort to analyse the above problem, Robertson [32], making many simplifying assumptions, formulizes the problem and obtains an equation of 18th degree in wave number k for these oscillations. The formulation has its value only in that, if it were solvable, it would predict the existence of many modes as observed by Donahue and Dieke.

A more systematic approach was then to study striations by transient methods. In this respect extensive investigations have been made by Pekarek [21-28] who studied the growth of striations by introducing an external perturbation at the cathode end of a homogeneous unstriated positive column which gave rise to the production of what he called the wave of stratification. In an analysis intended to justify this observation, Pekarek initially formulized the problem [23] which led to a solution that qualitatively predicted the existence of the wave of stratification.

In another transient study of striations Neusel and Silver [18], using a high voltage pulse to ionize the gas at high peak currents, obtained results in agreement with those obtained by Pekarek [26], even though they made their investigation under prebreakdown rather than on the positive column.

Still another investigator [13], in an effort to obtain the velocity of the positive ions in a discharge under prebreakdown, obtained results in close agreement with the above observations. It will be seen that this observation must have been an independent method of determining the velocity of the wave of stratification.

It will be seen that the initial theoretical analysis mentioned above [23] predicts two kinds of waves, a slow and a fast one, of which the above investigators make observations of the former, the slow wave of stratification.

In the present investigation observations are made of the fast wave of stratification at the onset of ionization. The results are in close quantitative agreement with the results of a theoretical analysis [27] made, again for the case when the positive column is externally perturbed. The assumptions of the analysis leads to results for fast striations.

This observation together with those previously discussed suggest that there is perhaps an inter-relationship among the parameters of striations occuring at the onset of ionization, during ionization growth in prebreakdown and in the positive column of a discharge. It further suggests that perhaps striations start, under ordinary circumstances, immediately after ionization begins. It can thus be conceived that for a study of the origin and growth of striations, its growth must be observed at various phases of development of ionization — the onset, the whole period of prebreakdown, and finally the glow — and all the observations studied for inter-relationships. This idea — the systematic observation of the growth of striations — is an important outcome of the present work and will be discussed in further detail in Chapter IV.

CHAPTER II

GENERAL CONSIDERATIONS

Introduction

A description of various modes of striation under several conditions of current and pressure in a steady-state glow discharge, as observed by Donahue and Dieke [3], is briefly outlined. A discussion of a theoretical analysis of this complicated problem, attempted by Robertson [32] is given. The formulation of the problem leads to an equation of 18th degree in k, the phase constant of the striation modes, which, if it were possible to solve, would lead to solutions of the frequency of the various modes of striation observed by Donahue and Dieke. Although the analysis qualitatively explains the existence of the modes, it gives no quantative explanation of the observations on striations, nor does it give any clues as to the origin or the temporal growth of striations. Pekarek, in a series of papers [21-28] tackles the latter problems theoretically and experimentally. For his work he uses the method of artificially perturbing the plasma of the positive column and observing the propagation of what he calls, the wave of stratification. The results of his final analysis are in close agreement with his experimental observations under typical conditions. Further, they are of the same order of magnitude as the observations made in this investigation, as will be seen in the following chapters.

Donahue and Dieke's Observations of Striations in a Steady-State Glow Discharge

The simplest conditions which can prevail in a glow discharge are usually taken to be those in which the positive column is homogeneous, and the current is constant. It is well known, however, that such conditions are rarely met and various modes of oscillation are so common that any theory which neglects them is defective in some essential way [3,23]. Nevertheless, thus far no theory has thoroughly explained the existence of these so called striations.

It is appropriate first to describe the nature of the striations in the positive column of a glow discharge and then discuss the most significant attempts in explaining the phenomena leading to these oscillations. The most noteworthy experimental work yet to explain the nature of the striations is carried out by Donahue and Dieke [3] who used photo-tubes and the oscilloscope for the observation of striations along the positive column.

The experimental arrangement consists of the glow discharge tube that is mounted horizontally. Beside it is an electron multiplier to which light is admitted from the narrow region of the glow through a slit. Output currents from the photo-tube circuit flow through a resistance at the input terminals of an oscilloscope. Thus the pattern on the cathode-ray tube screen gives the light output near a selected point in the glow discharge as a function of time.

Observations of the oscillations of the light intensity in general have been definitely periodic, although not quite sinusoidal. Besides the oscillations in the light intensity the apparatus in this method is provided

with means of observing the oscillations in voltage and current. Donahue and Dieke, in observing the latter oscillations, found that they have the same frequency and become irregular at the same time and in the same manner. Thus, the conclusion was drawn that they are related to the moving striations and that the two types of oscillations are different manifestations of the same phenomenon.

The voltage fluctuations can thus be used to trigger the driven sweep of the oscillograph which means that the sweep will always begin at the same instant of the cycle. The phase of the intensity oscillations are then observed to depend on the point in the tube from which the light comes. By changing the point of observation along the column, and looking at the time distance acceleration or retardation between two successive markers, the phase velocity of the light intensity oscillations can be measured. The method is thus to observe the intensity pattern at one point in the discharge, then to observe the same thing at a neighboring point and to repeat this until the whole length of the tube has been covered. In the meantime the discharge conditions are kept constant. In this way the phase velocity as well as the frequency and thus the wavelength of the light intensity oscillations can be determined.

To study the phenomena under as simple conditions as possible a monatomic gas, argon, is used in Donahue and Dieke's experiment.

The Basic Observations

Fig. 1 shows the ordinary dc characteristic of the glow discharge. The character of oscillations (stability, frequency, and velocity of propagation) are observed as function of current over a wide range of current.

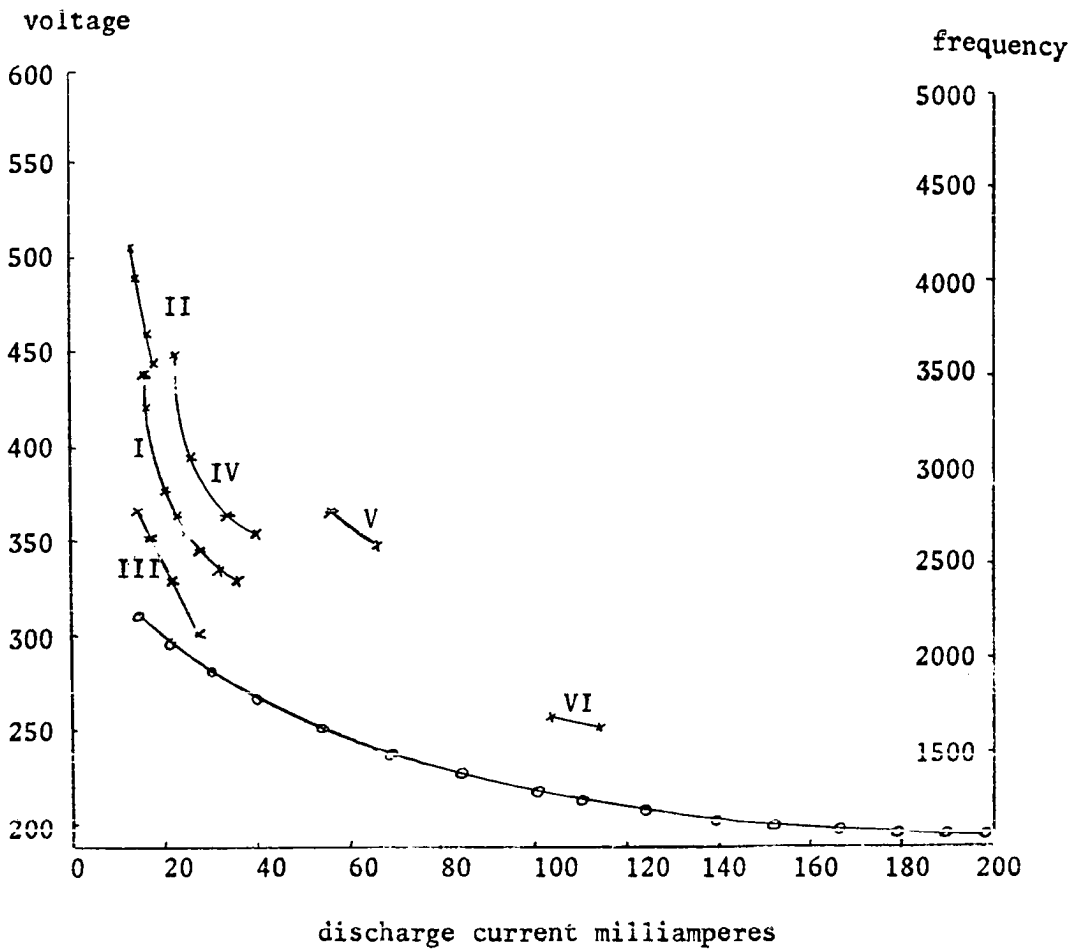

Fig. 1. Total discharge voltage o and frequency of oscillations × as functions of current for a glow discharge (Reference [3]: permission requested).

Fig. 1 gives also the observed frequency of the oscillations. It is immediately apparent that the various values do not lie on one continuous curve. When the current is increased the oscillations may become unstable and with further current increase, or sometimes even after a suitable waiting period at the same current, the oscillations become stable again but with a markedly different frequency. There are thus several modes of oscillations. For some values of current several modes can exist. Sometimes the oscillations move back and forth arbitrarily between two different modes and a confused picture arises. After some time the system usually will settle on a definite mode. For other current values stable oscillations apparently do not exist under any conditions. Regions in Fig. 1 where no frequencies are indicated are such regions of instability. There are values of current and pressure [3,26] where the discharge is entirely free from oscillations.

Fig. 2 shows that the intensity pattern may be quite different for different modes. Figures 2A and B represent mode III, 2C mode V, and 2D mode VI. The waveform of the intensity pattern may also change considerably when different parts of the tube are compared. It is usually more or less the same all through the positive column, but changes very greatly in character in the parts near the cathode. It is this behavior that Pekarek, as will be discussed later, utilizes to artificially perturb an unstriated positive column to observe the resulting strata, which he then explains theoretically and concludes that similar perturbations occur in the glow discharge leading to self-excited striations.

Figs. 3 and 4 show the appearance of the oscillations at various distances from the cathode. Donahue and Dieke define each of the maxima

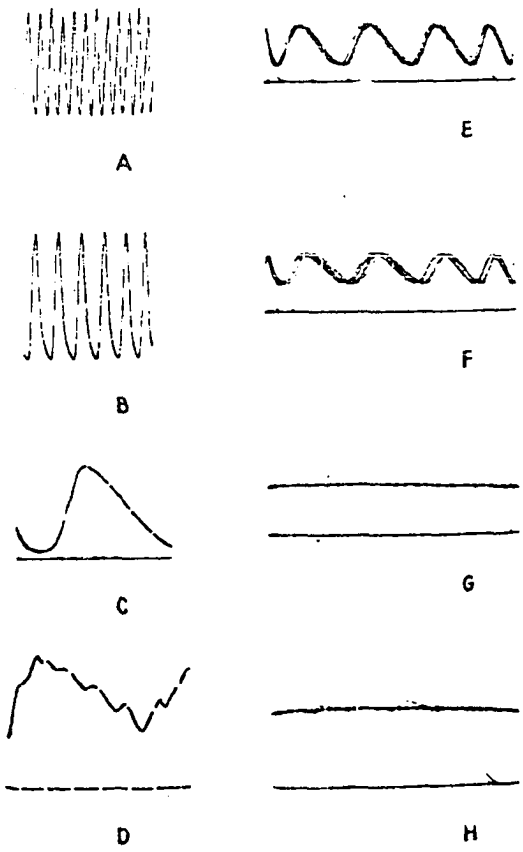

A: A typical voltage oscillation
B-H: Light intensity oscillations under different conditions of pressure and current at different distances from the cathode.

Fig. 2. Voltage and intensity oscillations in the glow discharge. Time markers are spaced 100 μsecs. apart. The lower trace in Figs. C-H is the zero line (Reference [3]: permission requested).

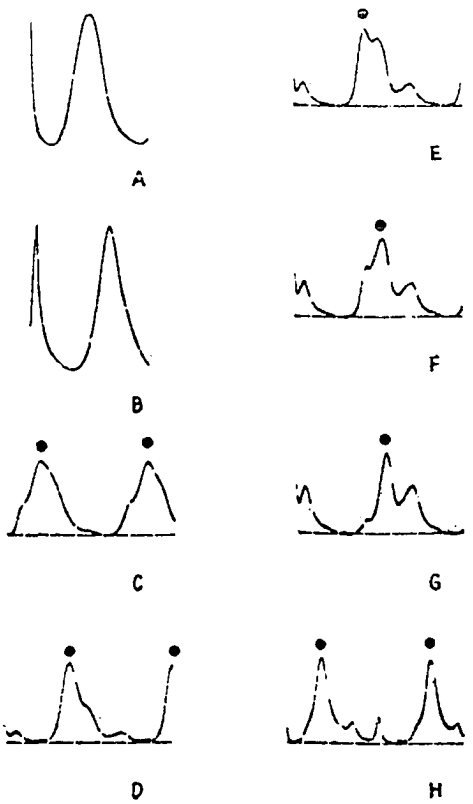

A,B: Light intensity at constant current I_1 at two different points along the discharge tube.
C-H: Light intensity at constant current I_2 at various distances from the cathode.

Fig. 3. Oscilloscope pictures of moving striations in argon, at constant pressure. The markers and the sweep are 100 μsecs. apart. The dot identifies the principal so called positive striations (Reference [3]: permission requested).

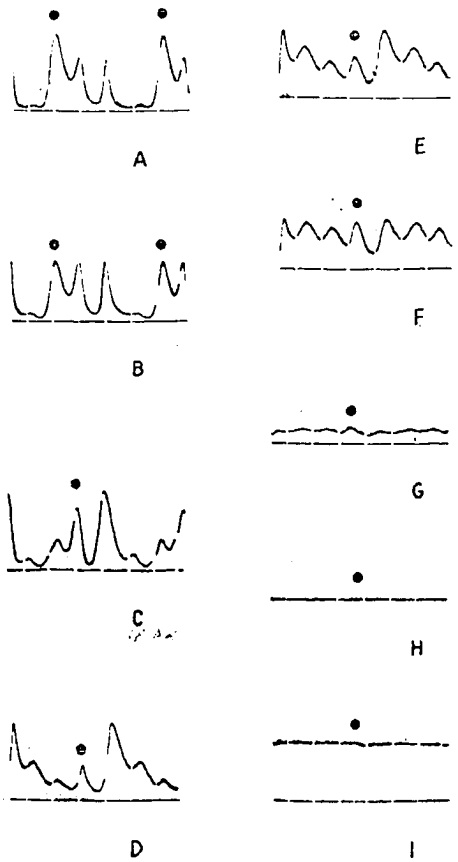

Fig. 4. Oscilloscope pictures of moving striations near the cathode in argon at constant pressure and constant current. Each waveform is the light intensity for a different point in the tube. A nearest to anode, I nearest to cathode (Reference [3]: permission requested).

visible on these traces a "striation". From the time scale on each trace the moment can be determined at which this particular striation reaches the spot of observation. From an inspection of the figures it is obvious that there are several striations of different character passing the spot of observation during each cycle. By comparing a whole set of pictures taken at different parts of the tube it is possible to trace the movement of each striation through the tube. A particular striation will not only move along the tube but may also change its amplitude and shape as it moves along.

At this point Donahue and Dieke summarize the result of observations by drawing curves, for each striation mode, of position of the observation versus the time when the maximum of that particular mode pases that point. They then observe that there are two types of striations. The slope of each curve indicates the velocity of the mode under consideration. The types of striations are dependent on the sign and value of the slopes of the appropriate curves and are called positive or negative striations. The negative striations are seen to move much faster than the positive ones. The situation is further complicated for a theoretical analysis by the fact that for each positive striation more than one so called negative striation exists. At 4.4 mm pressure, for example, there are nine negative striations for every two positive ones.

With the problem briefly described above, it is appropriate at this point to discuss the analysis made by Robertson, of striations under steady-state conditions. In formulation of the problem, Robertson considers most of the microscopic processes occuring in the discharge. This results in an equation of 18th degree in the wave number k of assumed oscillations which explains

the existence of the many modes observed. Unfortunately, this equation cannot be solved, and a method for observation of the temporal growth is more appropriate. Robertson's method is briefly explained.

Robertson's Theoretical Analysis of Striation Modes under Steady State Conditions

For this analysis a uniform (axially) positive column is considered first and stability conditions studied. Using the same basis of analysis, time and space variations are assumed from which striations are obtained.

The starting point for this analysis is the following equation:

$$\dot{Y} = G - L, \tag{II-1}$$

where Y is the appropriately averaged concentration of the component under study, $\dot{Y}$ its time-derivative, G is the production rate of the component Y, and L its loss rate. At equilibrium, $\dot{Y} = 0$.

Eq. (II-1) for each of the components of the positive column may be written:

$$\dot{N} = F_1(N) + MF_3(N) + 1/2\ \alpha_1 M^2 - \gamma N - \alpha NP \tag{II-2}$$

$$\dot{P} = F_1(N) + MF_3(N) + 1/2\ \alpha_1 M^2 - \gamma P - \alpha NP, \tag{II-3}$$

$$\dot{M} = F_2(N) - MF_4(N) - \alpha_1 M^2 - \nu M^2 + \beta\alpha NP, \tag{II-4}$$

where N, P, and M are electron, positive ion, and metastable atom concentrations respectively. $F_1(N)$ is a function representing the rate at which ion pairs are produced by direct electron impact. It can be shown

[32] that this rate is a function of N alone by eliminating E dependence.

$F_2(N)$ is the rate at which metastables are produced by direct electron-atom interaction. The term $MF_3(N)$ represents the rate of ionization of metastables by electron interaction.

The term $MF_4(N)$ in Eq. (II-4) is the loss of metastables by electron impact. F_4 should resemble F_3 but always exceed in magnitude since not all electron processes which destroy metastables will yield ions.

The terms $\alpha_1 M$ represent ion pair formation and consequent metastable loss as a result of the interaction of two metastable atoms with sufficient total energy to produce one ion pair and one normal atom.

The terms γN, γP, and νM represent losses to the walls and, in the metastable case, deexcitation by collisions with gas atoms. The recombination terms αNP lead to a fraction β of recombined ions which become metastable.

The functions F_1, F_2, F_3, and F_4 have been found based on a method outlined by Druyvesteyn and Penning [4].

To avoid further complication photon processes are ignored.

In order that equilibrium stability may be readily obtained, it is assumed that $N=P$, and we let $N=N_0 + \delta N$, where zero subscripts indicate values at the equilibrium condition.

From Eqs. (II-2) and (II-4), expansion about singular points and elimination of equilibrium conditions gives a pair of equations of the form:

$$\dot{\delta N} = (\partial \dot{N}/\partial N)_0 \delta N + (\partial \dot{N}/\partial M)_0 \delta M, \qquad \text{(II-5)}$$

$$\dot{\delta M} = (\partial \dot{M}/\partial N)_0 \delta N + (\partial \dot{M}/\partial M)_0 \delta M, \qquad \text{(II-6)}$$

where again the zero subscript indicates evaluation at equilibrium point. Solutions of the form $\delta N = (\delta N)_0 e^{\Gamma t}$ and $(\delta M)_0 e^{\Gamma t}$ lead to the consistency condition

$$\Gamma^2 + b\Gamma + c = 0 \qquad \text{(II-7)}$$

where

$$b = -(\partial \dot{N}/\partial N)_0 - (\partial \dot{M}/\partial M)_0,$$

$$c = (\partial \dot{N}/\partial N)_0 (\partial \dot{M}/\partial M)_0 - (\partial \dot{N}/\partial M)_0 (\partial \dot{M}/\partial N)_0.$$

Stable solutions will occur if $b>0$ and $c>0$. An analysis, assuming constant current density, based on the form of the functions F_1, F_2, F_3 and F_4 shows that metastable dependent columns can be unstable if the singular point in the ion and metastable rate equations occurs at sufficiently high metastable concentration and in the proper ion concentration range. The possibility of such instability may arise from localized departures from equilibrium, and that those instabilities might be the cause of moving striations.

Moving Striations

To obtain wave motion, space and time dependent variables are used. Eq. (II-1) is written in much the same way except that the z dependence is no longer ignored in the divergence of the particle currents. The particle currents in the z direction are given by

$$Nv_N = -D_- \partial N/\partial z - \mu_- NE, \tag{II-8}$$

$$Pv_P = -D_+ \partial P/\partial z + \mu_+ PE, \tag{II-9}$$

$$Mv_M = -D_* \partial M/\partial z, \tag{II-10}$$

where the D's are the appropriate diffusion coefficients, the v's are the velocities in the z direction, and E the effective field strength in the z direction. Inclusion of the divergence terms in the rate equations, and the substitution $E = Je(\mu_+ P + \mu_- N)$, with J considered constant, gives

$$\dot{N} = D_- \partial^2 N/\partial z^2 + [\mu_+ \mu_- J(P\partial N/\partial z - N\partial P/\partial z)]/[e(\mu_+ P + \mu_- N)^2]$$
$$+ F_1 + MF_3 + 1/2\alpha_1 M^2 - \gamma N - \alpha NP. \tag{II-11}$$

$$\dot{P} = D_+ \partial^2 P/\partial z^2 + [\mu_+ \mu_- J(P\partial N/\partial z - N\partial P/\partial z)]/[e(\mu_+ P + \mu_- N)^2]$$
$$+ F_1 + MF_3 + \alpha_1 M^2 - \gamma P - \alpha NP, \tag{II-12}$$

$$\dot{M} = D_* \partial^2 M/\partial z^2 + F_2 + \beta\alpha NP - \alpha_1 M^2 - MF_4 - \upsilon M. \tag{II-13}$$

Let $$N = N_0 + \delta N; \quad P = P_0 + \delta P; \quad M = M_0 + \delta M, \tag{II-14}$$

where the equilibrium values, considered independent of time and space, are denoted by the subscript 0 and the departures from equilibrium are considered small. Simplifying the equations and substitutions of the type $\delta N = \delta N_0 \exp(\Gamma t + Kz)$, leads to the determinant

$$\begin{vmatrix} K^2D_- - \Gamma + KV_+ + (\dot{\partial N}/\partial N)_0 & (\dot{\partial N}/\partial P)_0 - KV_+ & (\dot{\partial N}/\partial M)_0 \\ (\dot{\partial P}/\partial N)_0 + KV_+ & K^2D_+ - \Gamma - KV_+ + (\dot{\partial P}/\partial P)_0 & (\dot{\partial P}/\partial M)_0 \\ (\dot{\partial M}/\partial N)_0 & (\dot{\partial M}/\partial P)_0 & (\dot{\partial M}/\partial M)_0 + K^2D_* - \Gamma \end{vmatrix} = 0, \quad \text{(II-15)}$$

where V_+ is the average positive ion drift velocity. This equation is cubic in Γ and of sixth degree in K. As a result of some simplifications certain useful results will be obtained.

Probably Eq. (II-15) is satisfied by some waves which increase exponentially, but physical reasoning requires that solutions be bounded so we let

$$\Gamma = j\omega \quad \text{and} \quad K = -jk, \quad \text{(II-16)}$$

where ω and k are assumed to be real. Eq. (II-15) may then be separated into real and imaginary parts. Each part is a relationship between ω and k, and these must be simultaneously valid. Elimination of ω between them gives rise to an equation of 18th degree in k. For each of the eighteen roots of this equation, a unique ω exists, so it is possible for Eq. (II-15) to lead to eighteen frequencies and wave numbers. Probably not all of the roots of the k equation are real, and those that are not are meaningless, since they contradict the original assumption.

Since the 18th degree equation in k is still beyond the reach of practicality, a further simplification is made. Assume $\delta M=0$, so that the equivalent of Eq. (II-15) becomes a 2×2 determinant,

$$\begin{vmatrix} -k^2D_- - j\omega - jkV_+ + (\dot{\partial N}/\partial N)_0 & (\dot{\partial N}/\partial P)_0 + jkV_+ \\ (\dot{\partial P}/\partial N)_0 - jkV_+ & -k^2D_+ - j\omega V_+ + (\dot{\partial P}/\partial P)_0 \end{vmatrix} = 0. \quad \text{(II-17)}$$

This is equivalent to the assumption that the metastables and normal atoms form a two-component gas, each of which is so populous that no rate equation need be written for either the metastable gas or the normal atom. Ions and electrons can be made from both gases, and rate equations are then written for only ions and electrons.

Separation of Eq. (II-17) into real and imaginary parts and neglecting the production and loss terms, there is obtained:

$$\omega^2 = (D_- D_+)\ k^4, \tag{II-18}$$

and

$$\omega = kV_+\ (D_- - D_+)/(D_- + D_+). \tag{II-19}$$

The phase velocity is $\omega/k = V_+$, approximately, since usually $D_- >> D_+$. To this same approximation,

$$k = V_+(D_- D_+)^{-1/2} = \mu_+ E_0 (D_- D_+)^{-1/2}, \tag{II-20}$$

$$\omega = V_+(D_- D_+)^{-1/2} = (\mu_+ E_0)^2 (D_- D_+)^{-1/2}. \tag{II-21}$$

The phase velocity is thus seen to be approximately the positive-ion drift velocity, and in the direction of the current flow, i.e., toward the cathode.

A similar result is obtained by S. Watanabe and N.L. Oleson using a different approach particularly in the problem of ion production and loss [40].

It is obvious that this analysis, even though it considers most of the processes occuring in the discharge, does not lead to any quantitative

explanation of the observations on striations, nor does it give any clues as to the origin or the temporal growth of striations. The latter problems are analysed fully in a series of papers by Pekarek [21,22,23,26,27.28]. They are briefly discussed in the following pages.

Pekarek's Analysis of the Origin and Growth of Striations in the Positive Column

Pekarek, based on the conception that it is difficult in self-excited striations to find the conditional dependence and temporal evolution of processes which cause the existence of moving striations, sets forth the method of artificial perturbations. He performs his experiments in inert gases. He introduces a pulse voltage in an unstriated positive column and makes observations of the transient response of the light intensity of the positive column and the discharge voltage. Pekarek observes, through taking photographs by means of a rotating mirror, that after the disturbance, striations arise in the positive column of the discharge; further, they originate earlier at the cathode end of the column and each has a finite lifetime which is longer for striations at greater distances from the cathode. In the self-oscillatory state, Pekarek concludes that this process, the successive production of the wave of stratification, repeats. The individual striations of these waves, however, follow each other and the separate waves of stratification cannot be observed in the self-oscillatory state. The perturbations caused by periodically repeating these waves are observed as pulses propagating in the direction from cathode to anode (negative striations in the terminology of Donahue and Dieke).

The properties of these waves are thus different from a sinusoidal wave.

After a brief description of the experimental observations using the method of artificial perturbations, the theoretical analyses made by Pekarek using two different approaches will be discussed. It will be shown how the two different methods of analysis each making different simplifying assumptions lead to solutions that justify the observations.

Pekarek's Solution of the Striation Problem

Figure 5 schematically depicts the stratification in the plasma of a positive column, typical for the successive production of striations in a

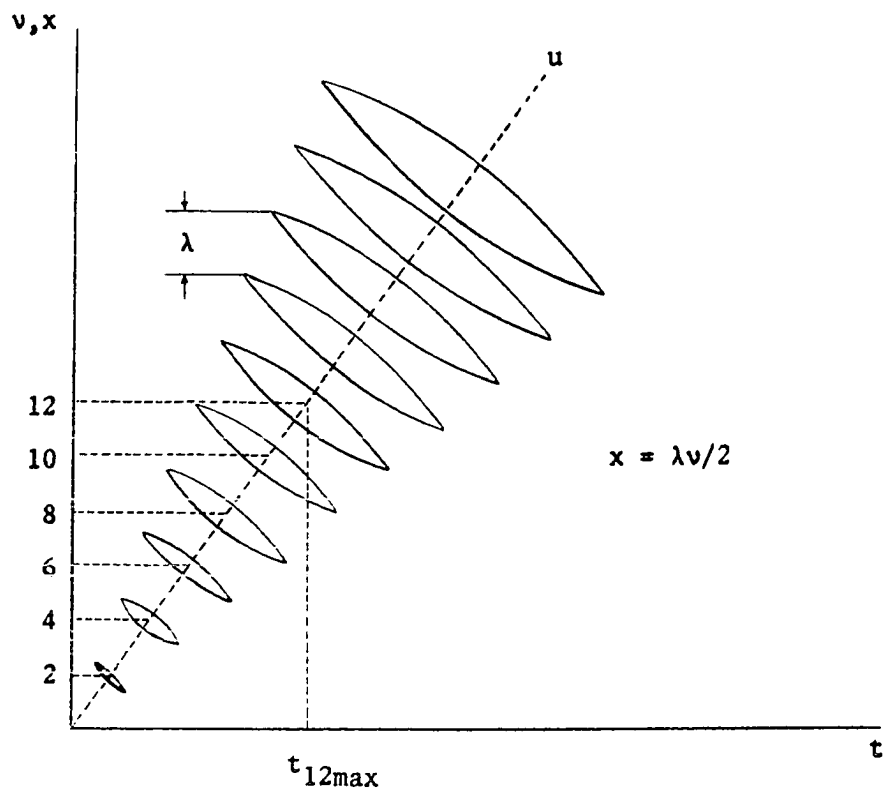

Fig. 5. Schematic plotting of the wave of stratification.

discharge in an inert gas. The time is from left to right, the direction of the axis of the discharge corresponds to the direction of the x-axis, the cathode is below, the anode is above.

The moving striations are shown by strong slanting lines. The scheme corresponds to the experiment when at a time $t=0$, a perturbation is introduced into the discharge by means of a voltage pulse, and this causes the successive production of striations in the positive column, which has originally been homogeneous. The first striation begins to appear at the cathode end of the column immediately after perturbation, then the second, then the third, and so on. Each striation appears somewhat later than the one before nearer to the cathode. If the behavior of any of the striations is considered, it is seen that at first the striation has a small intensity. This intensity gradually increases, reaches its maximum, again decreases, again decreases and finally the striation vanishes (the intensity of the striation is schematically shown in the figure by the thickness of the line). Each striation thus has a certain life-time which, as is obvious from the figure that actually corresponds to the situation found experimentally, is greater for striations at a greater distance from the cathode which were thus produced later.

Each striation attains a maximum amplitude at a certain time t_{max} after the instant of external perturbation. This time is greater the farther the striation is from the cathode. If the maxima of the amplitudes of the individual striations are joined up, a straight line is obtained, the slope of which corresponds to the velocity u of the propagation of the wave of stratification from the cathode to the anode (dotted in Fig. 5).

Corresponding places in neighboring striations are spacially distant from one another by a space period of the striations λ.

The oscillating process of the voltage on the discharge caused by the arrival of the wave of stratification in the anode region of the discharge has the same frequency.

Fundamental Concepts in Pekarek's Theory

The external perturbation, realized either by a sharp pulse applied to the external electrode in the neighborhood of the cathode end of the column, or by a steep step in the electric current of the discharge, causes a short-period increase in the electron temperature in the limited space on the cathode end of the column. This leads to a short-period increase in the number of inelastic collisions of the electrons with the atoms at this point. As a result of this, two different chains of processes take place.

Chain I. An increase in the number of inelastic collisions leads to an increase in the number of acts of direct ionization of the atoms by the electrons, and in the region of short period increase in electron temperature the concentration of current carriers of both signs increases. As a result of the greater mobility of the electrons a positive space charge caused by the excess of positive ions is produced in this region. This space charge gradually vanishes because the local excess of ions also disintegrates by diffusion but much more slowly than the increased concentration of electrons.

This process is shown schematically in the diagram in Fig. 6, the upper branch; $+\theta_v$ denotes the deflection (increase in this case) of electron temperature, $+n$, the increase in concentration of current carriers (of both signs), q, the space charge. The velocity of the disintegration of

the positive space charge by diffusion of the ions can be characterized by the time constant α or its inverse value, the relaxation period τ_1.

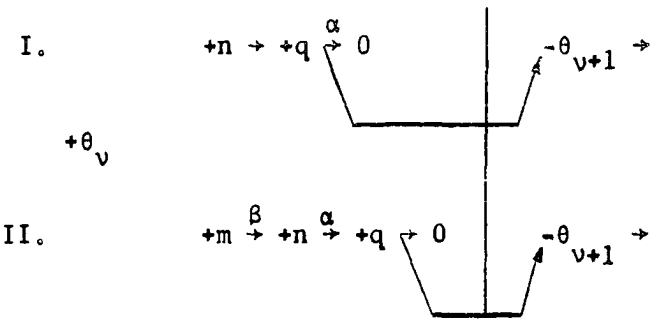

Fig. 6. Scheme of two chains of processes which can lead to successive production of striations.

Chain II. As a result of the short period increase in the electron temperature the concentration of the metastable atoms in the cathode end of the positive column is also increased by +m (Fig. 6 lower branch). The atoms in metastable state can be converted by a further collision with the electron into ion pairs. This process, which can be characterized by the time constant β or its inverse value, the relaxation period $\tau_2 = 1/\beta$, also leads to an increase in concentration of the current carriers at this point and thus to the production of a positive space charge which gradually disintegrates with the time constant α in the same way as in the case of Chain I.

Thus, Chain I is the cause of the production of a fast wave of stratification and Chain II of a slow wave.

The supplementary electric field caused by the criterion of a positive space charge in the cathode end of the column weakens the total electric

field on the anode side of this region. This leads to the criterion of a dark part of the striation because the electron temperature in this region, lying closer to the anode, decreases. The same processes as in the light region are repeated in the dark region but the deflections of the parameters of the plasma from the values corresponding to a homogeneous unstriated column now have opposite sign: the concentration of the ions and atoms in metastable states decrease, and a negative space charge is produced which causes an increase in the electric field on the anode side of the dark region. The electron temperature in this region increases and a light region of a further striation is thus produced.

According to this concept, therefore, each striation is composed of two relatively independent regions. The first, the light region, lying nearer to the cathode, is characterized by an increase in intensity of the processes forming the plasma and this is accomplished by an increase in the intensity of the radiated light. The second, the region of the striation lying closer to the anode, is produced by the creation of a positive space charge in the first region, and is characterized by a decrease in intensity of the given processes and by the creation of a negative space charge. The interaction, leading to the successive creation of light and dark regions, is realized by means of long range forces of the space charge. As a result of the asymmetry of the discharge maintained by a d-c current, the interaction is in the direction of the cathode to anode, in accordance with the direction of the drift of the ionizing electrons.

The so called wave of stratification can thus be interpreted as the gradual macroscopic polarization of the plasma of a positive column, the creation of characteristic "domains" with alternatively positive and negative

space charges. During the creation of this "domain structure" of the plasma there can come about a decrease in the power necessary for maintaining an equal current of the discharge and this is manifest in the amplification of the wave of stratification. Although even in the case when there is a decrease in the energy losses during the disintegration of the positive column into striations, the macroscopic polarization in an inert gas is unstable and if the perturbation which caused the first region at the cathode end of the column is not repeated, the striations again disintegrate. The localized space charge is thus again not maintained in the plasma if it is not periodically created by repeated perturbations.

The concept of the gradual polarization of the plasma of a positive column, of the creation of "a domain structure" with domains having an alternatively positive and negative space charge, while each region behaves as a relatively independent whole with its average space charge causing the creation of another region with opposite polarity, renders possible a simplified formulation of the theory of the gradual propagation of this polarization in plasma of a positive column. If it is considered that each such region is a closed whole in which the processes in question are concentrated leading to the creation of a space charge, and that the change in electric field caused by this space charge, is a phenomenon which only acts beyond the boundaries of this region and creates the condition for the production of another region, then for the theory of the successive production of striations the main question which must be solved is the time dependence of the creation of one region by the other, and their gradual disappearance.

In such a case it is possible to consider a value of the parameters θ, n, m, q for each such region, which is variable in time but averaged in

space, ascribe to each region a certain order number ν, beginning with $\nu = 0$ for the region on the cathode end of the column, and to formulate the problem as the finding of the time dependence of the parameters θ_ν, n_ν, etc. in the ν-th region caused by the time change in the space charge $q_{\nu-1}$ in the $(\nu-1)$-st region. Such a theory cannot explain the length of the spatial period λ, but one can expect it to explain and express the dependence of all the wave of stratification, measurable only in the transient state: the life time of the ν-th striation and its dependence on the order number of the striation, the velocity of propagation u of the perturbation, the ratio of the amplitudes of the neighboring striation and its dependence on the order number of the striations.

Formulation of Basic Equations

Referring to Fig. 5, always one certain x_ν corresponds to each maximum and minimum of the intensity of striations. The maxima of the light regions are denoted by the even subscripts $\nu = 0, 2, 4, \ldots$, and the minima of the intensity in dark regions by odd subscripts $\nu = 1, 3, 5, \ldots$

The analysis will then be started with the following assumptions:

1. The processes in the ν-th region are caused by the effect of the space charge in the $(\nu-1)$-st region.

2. The first light region on the cathode end of the positive column $(\nu = 0)$ is caused by the external short period perturbation.

3. The theory can be formulated as a theory of small deflections of the state of the plasma of the positive column from the homogeneous state.

4. The processes in each region can be characterized by average values in space and variable in time of the corresponding quantities (e.g.

electron temperature $T_\nu(t)$, concentration of metastable atoms $M_\nu(t)$ etc.).

The electron temperature in the ν-th region is denoted by

$$T_\nu(t) = T_0 + \theta_\nu(t) \tag{II-22}$$

where T_0 is the temperature in a homogeneous unstriated column. Similarly the concentration of ions is represented by

$$N_\nu(t) = N_0 + n_\nu(t) \tag{II-23}$$

and that of the metastable atoms by

$$M_\nu(t) = M_0 + m_\nu(t), \tag{II-24}$$

where again N_0 and M_0 are values of the appropriate concentrations at a homogeneous unstriated column. The increase (or decrease) in intensity of light i_ν emitted from the ν-th region

$$J_\nu(t) = J_0 + i_\nu(t) \tag{II-25}$$

can for a small value $\theta_\nu(t) \ll T_0$ be assumed proportional to the deflection of the electron temperature:

$$i_\nu = \xi\theta_\nu. \tag{II-26}$$

If θ is negative, a dark region of the striation is produced.

Equations will be developed that express the mutual relation of the individual quantities in the ν-th region for both Chains (I) and (II) in Fig. 6.

All the given processes of Chains (I) and (II) take place at a finite velocity, the resultant time course of the quantities being determined by the slowest of the processes.

In Chain (I) the slowest process is the disintegration of the positive charge by diffusion of the ions. The other processes (diffusion of electrons, attaining of the electron temperature after a change in the electric field) are in order of magnitude much faster. It suffices therefore to consider in Chain (I) only the velocity of the disintegration of the positive charge, characterized by the time constant α.

In Chain (II) the velocity of the decrease in the excess concentration of metastables β is a process at least as slow as the diffusion of the positive ions. To find the time course of the quantities it is therefore necessary to consider in addition to the velocity of the disintegration of the positive space charge also the velocity of the decrease in excess concentration of the metastable atoms, characterized by the time constant β.

The other processes are assumed infinitely fast in comparison with those given. The deflection of the electron temperature in the ν-th region is put directly proportional (without delay) to the magnitude of the space charge in the $(\nu-1)$-st region (to which the supplementary electric field in the ν-th region is proportional):

$$\theta_\nu(t) = -\xi' q_{\nu-1}(t) = -\eta' n_{\nu-1}(t). \qquad \text{(II-27)}$$

The proportionality of the charge q to the deflection in concentration of the ions n follows from neglecting the finite velocity of the diffusion of the electrons with respect to the velocity of the diffusion of the ions.

For the processes of Chain (I) the following equation is written:

$$dn_\nu/dt = A'\theta_\nu - \alpha n_\nu, \qquad \text{(II-28)}$$

i.e., the time rate of change in concentration of the ions in the ν-th region is a linear function of the increase (or decrease) in electron temperature at this point and of the magnitude of the change itself (with time constant α), with negative sign.

By substituting from (II-27) n_ν can be eliminated from this equation and the differential equation for the time dependence of the deflection of the electron temperature (and thus also the intensity of the radiated light, i_ν, or the charge concentration n_ν) in the ν-th region

$$d\theta_\nu/dt + \alpha\theta_\nu = - A\theta_{\nu-1}. \qquad \text{(II-29)}$$

For the case of Chain (II) with stepwise ionization one can write quite analogously

$$dm_\nu/dt = B'\theta_\nu - \beta m_\nu \qquad \text{(II-30)}$$

$$dn_\nu/dt = \gamma m_\nu - \alpha n_\nu, \qquad \text{(II-31)}$$

where B' is a constant expressing the linearity of the creation of

the metastable atoms to the increase in electron temperature, in a similar way as A' in (II-28); β, the time constant of the disintegration of increased concentration of metastable atoms; α, the time constant of the disintegration of the positive space charge; $\gamma \leq \beta$, a constant expressing the probability of the creation of an ion pair during the disappearance of the metastable atom. (The disappearance of the metastable atom takes place in various ways. Either it is ionized by another collision and an ion pair is produced, or the metastable atom transfers energy by collision of a second kind to an electron or to another atom, or to the wall of the tube, or it is transferred by collision to another atom, or to the walls of the tube, or it is transferred by collision with an electron or atom to the non-metastable state with the following instantaneous emission of the light quantum. Only the first process, characterized by the constant γ is effective in creating a space charge. The velocity β of the disintegration of the excess of metastable atoms is on the other hand determined by the sum of all the processes leading to the disappearance of the metastable atom. Therefore $\beta \neq \gamma$.)

By eliminating m_ν and substituting from (II-27) for n_ν, an equation for the deflection of electron temperature $\theta_\nu(t)$ is obtained:

$$d^2\theta_\nu/dt^2 + (\alpha+\beta)d\theta_\nu/dt + \alpha\beta\theta_\nu = -B_0\theta_{\nu-1} \qquad \text{(II-32)}$$

where $B_0 = \eta'\beta B'$.

Eqs. (II-29) and (II-32) are systems of ordinary linear differential equations with constant coefficients from which the course of $\theta_\nu(t)$ can be calculated in an arbitrary ν-th place, if the time dependence of $\theta(t)$ is known for $\nu = 0$.

Solution of Equations of Successive Production of Striations

System (I) with the Single Slow Processes in Chain

It is possible to express the initial conditions approximately by a delta function

$$\theta_0(t) = a_0\delta(t). \qquad \text{(II-33)}$$

The course of the change in electron temperature $\theta_\nu(t)$ is an arbitrary ν-th region is thus uniquely determined by solving the system (II-29).

By the successive application of the two-sided Laplace transform in conjunction with the initial conditions, Eq. (II-33), there results, for the transform of the deflection of the electron temperature in region ν,

$$\theta_\nu(s) = (-A)^\nu a_0\alpha(s/\alpha)/(1+s/\alpha), \qquad \text{(II-34)}$$

and for $\theta_\nu(t)$

$$\theta_\nu(t) = (-A)^\nu a_0\alpha\,[1/\Gamma(\nu)](\alpha t)^{\nu-1}e^{-\alpha t}, \qquad \text{(II-35)}$$

This is the desired dependence for the course of the deflection of the electron temperature θ in the ν-th region for the initial condition (II-33).

Due to the fact that the change in intensity of the light emitted from the same region is put proportional to the change in electron temperature

(Eq. II-26), the expression on the right side of (II-35) simultaneously expresses the time dependence of the change in the light intensity in the ν-th region of the wave of stratification $i_\nu(t)$:

$$i_\nu(t) = (-A)^\nu b_0\, \alpha[1/\Gamma(\nu)]\, (\alpha t)^{\nu-1} e^{-\alpha t}, \qquad \text{(II-36)}$$

where $b_0 = a_0\xi$.

The time dependence of the electron temperature θ_ν (or light intensity i_ν) for $\nu = 2, 4, 8, 16$ is plotted in Fig. 7 for the value of the parameter $A = 1$. Each of the given curves corresponds to the course of the light intensity of the light region of the striation (even ν). The figure clearly shows the displacement of the maxima of the individual curve θ_ν for increasing ν to the right. This corresponds to the delay in the maximum values of the light intensity in the wave of stratification with growing order number of the region. Fig. 7 also clearly shows the increase in width of the curves for $\theta_\nu(t)$ with growing order number of the region, which corresponds to the increase in the lifetime of the regions with growing order number.

The values of the maxima of the individual curves in Fig. 7 decrease with growing order number of the region ν. This corresponds to the attenuation of the wave of stratification and is connected with the choice of the parameter $A = 1$ (i.e., the transfer of perturbation from one region to the other is not amplified). For $A>1$ the amplitudes of the individual curves $\theta_\nu(t)$ can increase with growing order number.

The values of $\theta_\nu(t)$ are positive for even ν, and negative for odd ν. This expresses the alternating of the light and dark regions. In the

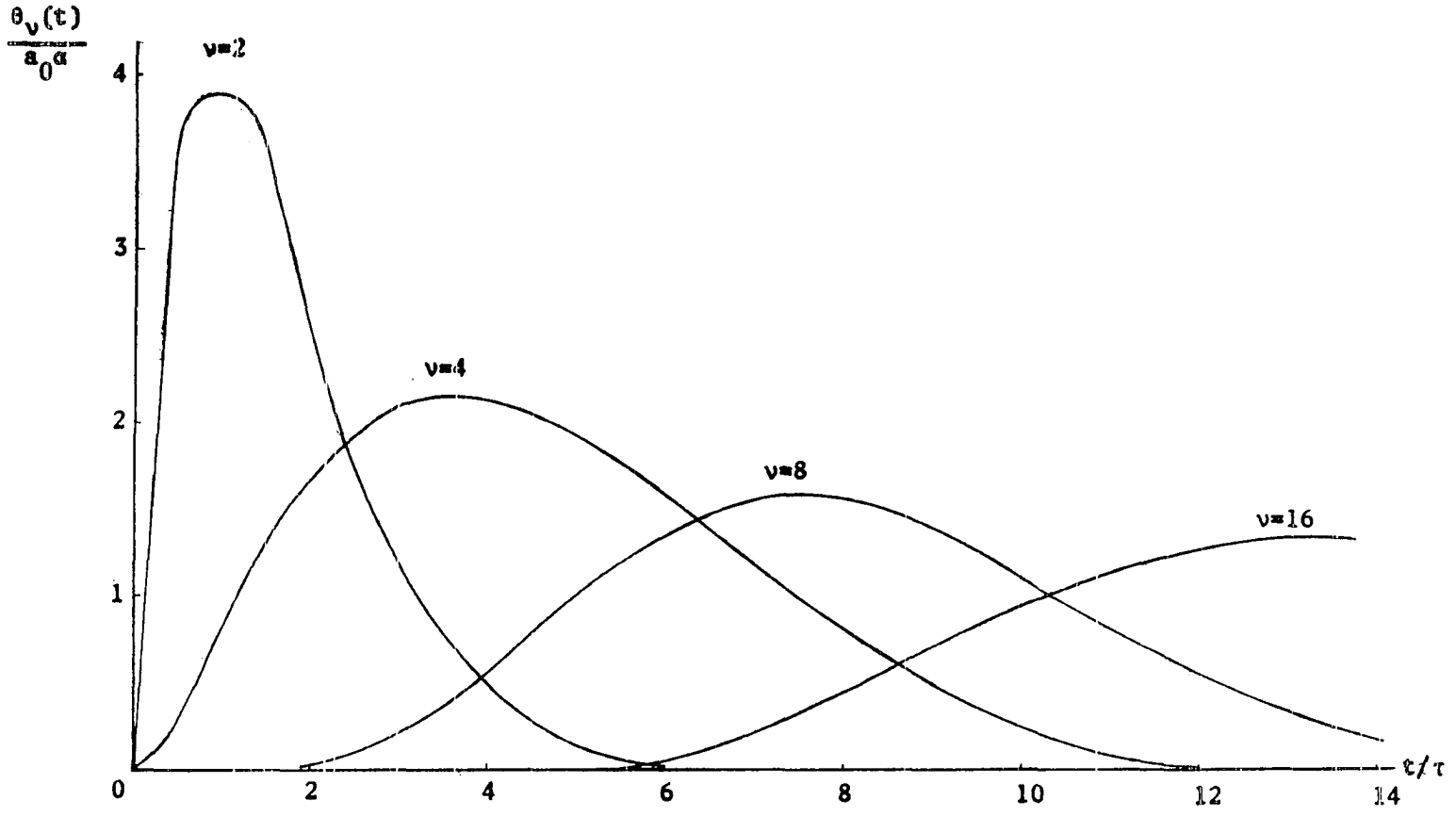

Fig. 7. Course of light intensity $i_\nu\theta$ in ν-th region for ν= 2,4,8,16 as a function of time, t/τ.

following, developments about values of $\theta_\nu(t)$ are considered.

Eq. (II-35) enables one to obtain some inter-relationships among the parameters of the wave of stratification analytically. For this purpose ν is considered a continuous variable, and instead of $\theta_\nu(t)$, $|\theta_\nu(t)|$ is taken.

First by putting $d\theta_\nu/dt = 0$, the following relation is obtained for the dependence of the period of maximum on the order number of the region

$$t_{\nu max} = (1/\alpha)(\nu-1) = \tau_1(\nu-1). \qquad \text{(II-37)}$$

The period of maximum is therefore proportional to the relaxation period τ_1.

Since, from Fig. 5, it holds that $\nu = x/(\lambda/2)$, then t_{max} is given by

$$t_{max} = \tau_1[x/(\lambda/2) - 1]. \qquad \text{(II-38)}$$

It is thus clear that the derivative

$$(dx/dt)_{t_{max}} = d[(\lambda/2)(t/\tau_1) + \lambda/2]/dt \qquad \text{(II-39)}$$

is equal to the velocity of propagation of the wave of stratification u. Due to the linear relation between t_{max} and $\nu(x)$ this velocity is constant, i.e., it does not depend on $\nu(x)$. The velocity of propagation of the wave of stratification u is thus inversely proportional to the relaxation time τ_1.

For the computation of the lifetime of striations, the width of the curve $|\theta_\nu(t)|$ between the inflexion points is taken. This is found, after taking the derivative, to be

$$\Delta t_{inflex} = (2/\alpha)(\nu-1)^{1/2} = 2\tau_1 (\nu-1)^{1/2}. \qquad \text{(II-40)}$$

The width in the points of the inflexion thus increases with $(\nu-1)^{1/2}$ and is again proportional to the relaxation period τ_1.

The maximum value of $|\theta_\nu(t)|$ occurs for $t = t_{max}$ where $\theta_\nu(t)>0$ for ν even, and $\theta_\nu(t)<0$ for ν odd. By substituting (II-38) into (II-35) there is obtained for these maximum (minimum) values

$$(1/a_0\alpha)\theta_\nu(t_{max}) = (-A)^\nu(\nu-1)^{\nu-1}[1/\Gamma(\nu)]e^{-(\nu-1)}. \qquad \text{(II-41)}$$

When this dependence is plotted for values of $A\leq 1$, it will be seen that $|\theta_\nu(t_{max})|$ decreases as a function of ν in a monotone manner with increasing ν. This corresponds to attenuation of the wave of stratification. For $A>1$ the maximum values at first decrease, attain a minimum and then permanently increase for increasing ν.

It is thus seen that this theoretical analysis gives an excellent qualitative picture of the experimental observations discussed previously. However, because of the existence of such unmeasurable parameters as α, and A in the solution, it is not possible to make any quantitative predictions. Pekarek analyses the same problem in a more conventional way making assumptions that are different from those in the above analysis. His analysis by this method leads to solutions which are independent of the initial

conditions, and this is consistent with a series of experiments performed by introducing an absolutely aperiodic (in time and space) local disturbance in the plasma of the positive column [24,25]. Pekarek shows that the plasma of the positive column essentially differs from the majority of other continuous media, in which the spatial periodicity is due to the time periodicity of the source. He shows that self-excited moving striations result from a superposition of repeated disturbances and thus concludes that if the specific characteristic property of the plasma, namely the development of periodicity after an aperiodic disturbance, and the resulting mechanism of the production of striations, can be physically explained, the nature of self-excited moving striations will thereby also be explained.

Based on the results of his experiments in the transient regime in which he has shown that the basic phenomena of the production of striations can be excited at any point of the plasma [25], and that the influence of the boundary regions of the discharge and the external circuits is subordinate and is apparent mainly in the case of self-excited striations [27], Pekarek, for the analysis of the production of striations resulting from an aperiodic perturbation in the plasma, considers the processes in the plasma of the positive column.

He then concludes that the following three phenomena are the most important for the physical mechanism of the production of striations:

a) The dependence of the rate of production of ion pairs (ionization coefficient) on the mean kinetic energy (temperature) of the electrons and thereby also on the intensity of the local electric field.

b) The production of a positive (or negative) space charge at the point of increased (or decreased) concentration of ion pairs. The diffusion

coefficient of electrons in the axial direction is much larger than the diffusion coefficient of ions ($D_- >> D_+$), and the electrons thus tend to remove local deviations in concentration much more quickly than positive ions. At the point of increased (or decreased) concentration of ion pairs an excess (or lack) of positive ions and hence a positive (or negative) space charge is thus produced.

c) The creation of additional electric fields, due to the creation of space charges, as described by Poisson equation.

In this method, in addition to the time t only one other independent variable is considered, namely, the space coordinate x in the direction of the discharge axis. Here the influence of the walls on the striation parameters are neglected because due to the very nature of striations, the problem can be handled as a one-dimensional problem.

The basic processes are then mathematically formulated. For this purpose the positive direction of the x-axis is chosen from the anode to the cathode and the origin $x=0$ at the point of the positive column to which the exciting impulse is applied. The basic equations are formulated for small deviations of the dependent variables E, N_+, N_- (electric field, concentration of positive ions and electrons, respectively) from their values in the equilibrium state. It is thus assumed that

$$E = E_0 + e, \qquad |e| << E_0, \tag{II-42}$$

$$N_+ = N_0 + n_+, \qquad |n_+| << N_0, \tag{II-43}$$

$$N_- = N_0 + n_-, \qquad |n_-| << N_0. \tag{II-44}$$

If the charge of an electron is denoted by q_0 and the slope of the dependence of the ionization coefficient on the electric field for an equilibrium value of the field E_0 by $z' = (\partial z/\partial E)_{E_0}$, then the equations

$$\partial e/\partial x = q_0 n_+, \tag{II-45}$$

$$\partial n_+/\partial t = z' N_0 e \tag{II-46}$$

include in a simple way all the three above-mentioned basic processes: process (a) is expressed by Equation (II-46), where it is assumed that the change in the electric field in the plasma causes a proportional change in the mean kinetic energy of the electrons instantly and in the same place. For process (b), the diffusion coefficient (and mobility) of the positive ions in the electric field is regarded as zero: on the other hand, the diffusion coefficient of the electrons is put equal to infinity (Debye length $l_D = \infty$), so that the deviations of the electron concentration from the equilibrium state are immediately removed and $n_- = 0$. In the Poisson equation (II-45), expressing process (c) therefore, only the deviation of the positive ion appears on the right side.

The initial condition is chosen in the form of a step function in the ion concentration

$$n_+(x,0) = n_0 u(x). \tag{II-47}$$

This is shown schematically in Fig. 8a. This space distribution of $n_+(x,0)$, corresponds best, for the simplified case of $D_- = \infty$, to the real situation

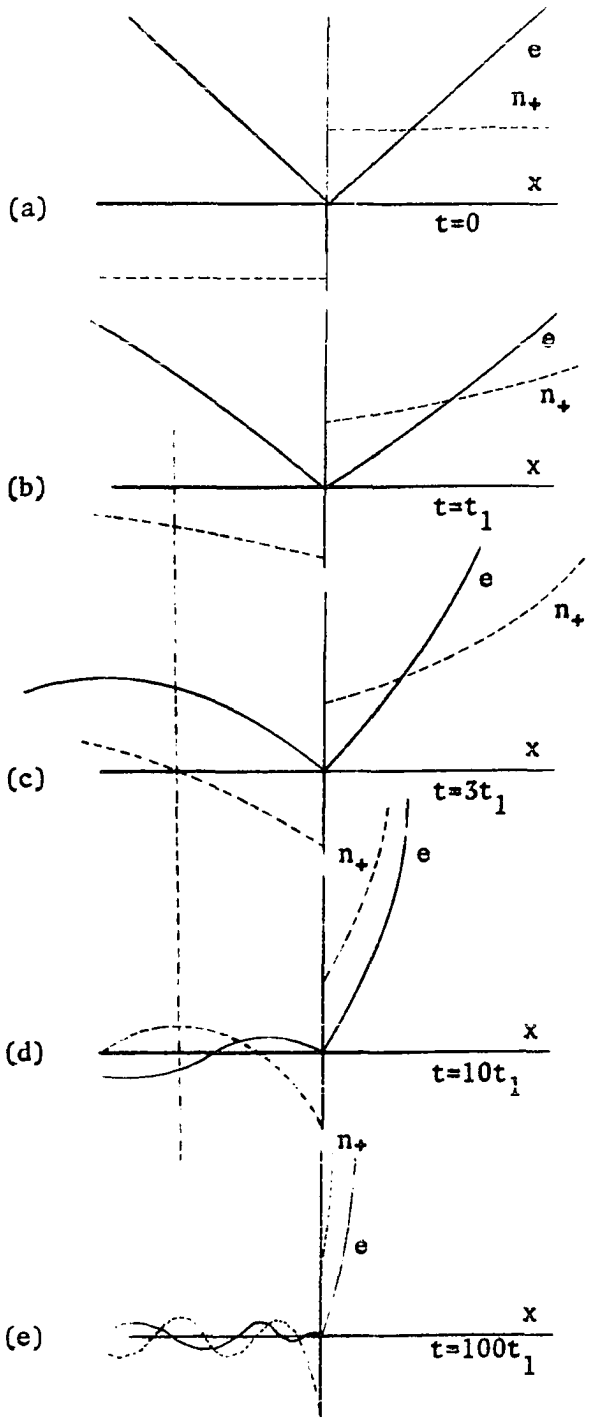

Fig. 8. Course of solutions (II-48) to (II-51) for the deflection from equilibrium of positive ion concentration n_+ and electric field e as a function of x for five values of t.

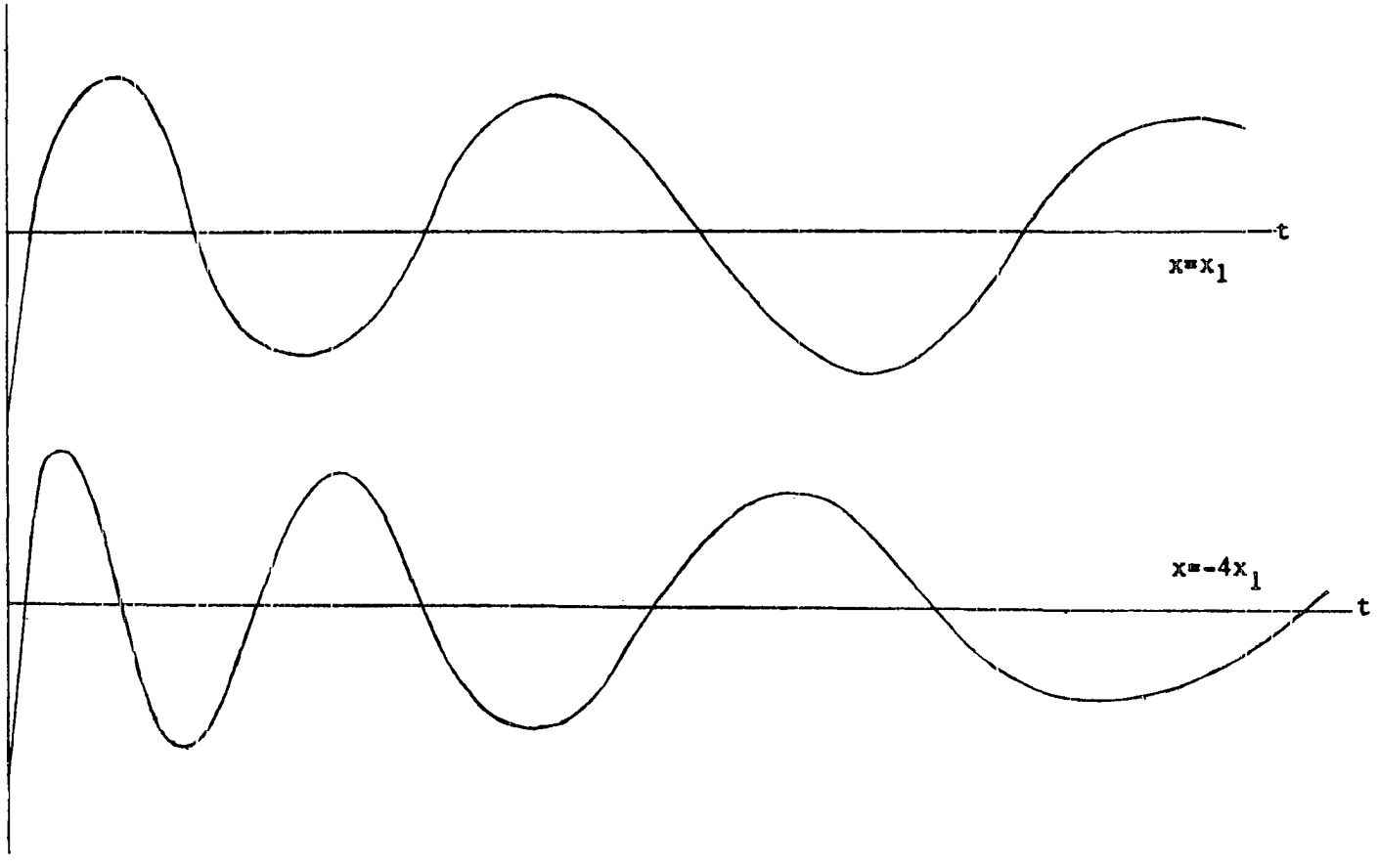

Fig. 9. Time dependence of deflections of concentration of positive ions (n_+) according to solution (II-50) at two different distances from point of disturbance.

in the experiment of local excitation of a wave of stratification: the short voltage pulse applied to the external electrode causes for a very short time-interval an increase of the electric field on one side of the point of disturbance and its decrease on the other side. The change in electric field causes the quantity n_+ to have the course shown in Fig. 8b. This distribution remains the same immediately after the exciting pulse is over. This moment is then chosen as $t = 0$. To the above dependence $n_+(x,0)$ corresponds according to Eq. (II-45) the dependence $e(0,0) = 0$. The solution of the system of equations (II-45) and (II-46) for the given initial conditions has the following form [37]

for $x>0$,

$$n_+ = n_0 I_0 [2(q_0 N_0 z')^{1/2} (xt)^{1/2}], \qquad \text{(II-48)}$$

$$e = -n_0 (q_0/N_0 z')^{1/2} (x/t)^{1/2} I_1 [2(q_0 N_0 z')^{1/2} (xt)^{1/2}], \qquad \text{(II-49)}$$

and for $x<0$

$$n_+ = -n_0 J_0 [2(q_0 N_0 z')^{1/2} (-xt)^{1/2}] \qquad \text{(II-50)}$$

$$e = -n_0 (q_0/N_0 z') (-x/t)^{1/2} J_1 [2(q_0 N_0 z')^{1/2} (-xt)^{1/2}], \qquad \text{(II-51)}$$

where I_0, I_1, J_0, and J_1 are modified Bessel functions and Bessel functions of the first kind.

It may be seen that the quality of the solution is not caused by the special choice of initial conditions and integration constant. For example, the change in polarity of the initial course of the function $n_0(x,0)$ would result in a change in the sign of n_+ and e but the solution

would otherwise be the same. For other aperiodic initial and boundary conditions the solution would, as a rule be more complicated but in any case the course of the quantities e and n_+ would be described by an aperiodic function for $x>0$ and by an expression containing an oscillating Bessel function for $x<0$.

The curve of solution of Eq. (II-48) to (II-51) for n_+ and e is shown in Fig. 8a to e for five different values of the variable t. It is seen that the idealized system of equations (II-45) and (II-46) gives even for an aperiodic initial condition a solution, which, in agreement with experiment [23] has an oscillating character only on one side of the place of disturbance, i.e., in the direction towards the anode ($x<0$), in which the wave of stratification is known to propagate. In the cathode direction ($x > 0$) the solution of Eqs. (II-45) and (II-46) is a monotone function in time and space.

Fig. 9 shows the time dependence $n_+(t)$ in two different points x_1 and x_2 ($|x_2|>|x_1|$). It is seen that the dependence is not periodic in the mathematical sense since the oscillation frequency is not constant and decreases with increasing time. Analogously, it is obvious from Fig. 8e that the wavelength (length of striation) also does not remain constant but increases with distance from the disturbance. The individual maxima shift towards the place of disturbance with time. This is also seen from Fig. 10, where the curve of the maxima (full lines) and minima (dashed lines) of the dependent variable $n_+(x,t)$ is plotted as a function of both independent variables x and t.

This picture conforms to the picture found experimentally, as previously discussed and shown in Fig. 5. However, in order to be able to utilize this

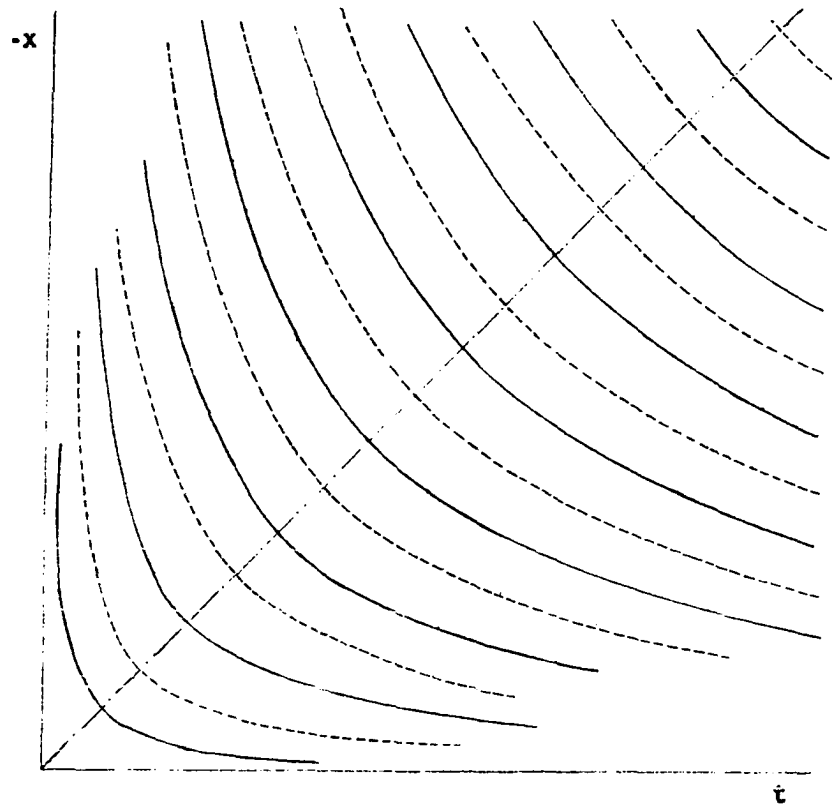

Fig. 10. Curves of maxima (———) and minima (----) of deflections of concentration of positive ions (n_+) according to solutions (II-50) as a function of time and distance from disturbance.

theory for experimental observations, a further modification is made by using the assymptotic relation valid for $y>>1$,

$$J_0(y) = (2/\pi y)^{1/2} \cos (y-\pi/4). \qquad \text{(II-52)}$$

The solution of (II-50) is obtained in the assymptotic form

$$\begin{aligned} n_+(x,t) &= [2/(-\pi a)]^{1/2}\cos [a(-xt)^{1/2} - \pi/4]/(-xt)^{1/4} \\ &\approx [2/(-\pi a)^{1/2} [\cos \phi(x,t)]/(-xt)^{1/4} \end{aligned} \qquad \text{(II-53)}$$

where $a = (q_0 z' N_0)^{1/2}$ and $\phi(x,t) = [a(-xt)^{1/2} - \pi/4]$.

Thus, the length of the striation can be expressed as a continuous function of the variables x and t:

$$\begin{aligned} \lambda(x,t) &= 2\pi/(d\phi/dx) \\ &= 2\pi/ (\partial/\partial x)[a(xt)^{1/2} - \pi/4] \\ &= (4\pi/a)(-x/t)^{1/2}. \end{aligned} \qquad \text{(II-54)}$$

For the point with λ = constant = λ_0, there is obtained

$$x = -(a^2/16\pi^2)\ \lambda_c^2 t = u_\lambda t, \qquad \text{(II-55)}$$

so that u_λ, the velocity of the wave of stratification is

$$u_\lambda = -a^2\lambda_c^2/16\pi^2. \qquad \text{(II-56)}$$

This equation can be used to find values of the velocity u_λ under typical conditions. This is done in Chapter IV where Pekarek's results are compared with those found in the present investigation.

CHAPTER III

THE PRESENT WORK - OBSERVATION OF FAST STRIATIONS

Introduction

It was seen in Chapter II that the complexity of observations made in a steady state striated glow discharge and the impossibility of the solution of the problem formulized theoretically led those working on the problem to simplify it by following the growth of striations. Towards this aim, it was explained in Chapter II that Pekarek introduced external perturbations in a homogeneous unstriated glow and observed the production of what he called the wave of stratification.

Without perturbing the ionized gas, and during prebreakdown instead of under glow conditions, Neusel and Silver [18] obtained results comparable to those of Pekarek [26] for what will be seen to be slow striations. In an effort to determine the velocity of positive ions during prebreakdown in a discharge, another worker [13,20] using a different technique, independently obtained results that, as will be seen later, are believed to be slow striations discussed above.

In the present investigation, observations are made, at the onset, of what is shown to be the fast striations. The phenomenon justifying the observations is based on the fundamental concepts of Pekarek's theory [23].

The problem is reformulized and an equation is obtained in terms of density n of the ion pairs instead of electron temperature as carried out by Pekarek. The picture thus obtained which conforms to that of Fig. 5, is used to justify the observation and the technique. This theory cannot be used for quantitative comparison with the results but the results are in close agreement with another theory developed by Pekarek [27] for the case of external perturbation of a homogeneous positive column.

Derivation of a Differential Equation in n_ν for the Wave of Stratification

For the equation n_ν, the density of ion pairs at any region ν, Eqs. (II-27) and (II-28) are utilized. These equations are as follows:

$$\theta_\nu(t) = -\eta' n_{\nu-1}(t), \tag{III-1}$$

$$dn/dt = A'\theta_\nu - \alpha n_\nu. \tag{III-2}$$

Substituting (III-1) into (III-2), there results

$$dn_\nu/dt + \alpha n_\nu = -\eta' A' n_{\nu-1}(t). \tag{III-3}$$

Equation (III-3) is similar to Eq. (II-29) of Chapter II for electron temperature $\theta_\nu(t)$. For the problem of exciting the wave of stratification by an external sudden perturbation, the initial condition can be approximately expressed in the zero-th region by the Dirac delta function. Thus,

$$n_0(t) = a_0\,\delta(t). \qquad \text{(III-4)}$$

The course of the change in $n_\nu(t)$ in any arbitrary ν-th region is uniquely determined by solving the system (III-3) subject to initial condition (III-4). The solution to this system can be found by the successive application of two-sided Laplace transform [37]:

$$N_\nu(s) = s\int_{-\infty}^{\infty} e^{-st} n_\nu(t)dt, \qquad n_\nu(t) = 0 \text{ for } t<0. \qquad \text{(III-5)}$$

A system of algebraic equations for the transformed function $N_\nu(s)$ can thus be found:

$$sN_\nu(s) + \alpha N_\nu(s) = -\eta' A' N_{\nu-1}(s). \qquad \text{(III-6)}$$

This results in

$$N_\nu(s) = [-\eta' A' N_{\nu-1}(s)]/(s+\alpha)$$

$$= -(\eta' A'/\alpha)[N_{\nu-1}(s)]/(s/\alpha+1)]. \qquad \text{(III-7)}$$

This is the recurrent relation for N_ν. By substitution an expression for N_ν expressed by initial condition N_0 can be obtained as:

$$N_\nu(s) = (-B)^\nu N_0(s)/(s/\alpha + 1)^\nu, \qquad \text{(III-8)}$$

where

$$B = \eta' A'/\alpha, \tag{III-9}$$

and

$$N_0(s) = s \int_{-\infty}^{\infty} n_0(t)\, e^{-st} dt, \tag{III-10}$$

$$= s \int_{-\infty}^{\infty} a_0(t) e^{-st} dt = s a_0, \tag{III-11}$$

and thus

$$N_\nu(s) = (-B)^\nu a_0 \, (s/\alpha)/(s/\alpha+1)^\nu. \tag{III-12}$$

The inverse Laplace transform of the above is

$$n_\nu(t) = \alpha a_0 \, [(-B)^\nu (\alpha t)^{\nu-1}/\Gamma(\nu)] e^{-\alpha t} \tag{III-13}$$

which is the same as that for $\theta_\nu(t)$ obtained in a similar way. The shape of the plots of $n_\nu(t)$ versus time for this expression has the same shape as that given in Fig. 7 in Chapter II for $B<1$. It thus conforms to the picture given for the wave of stratification in Fig. 5, Chapter II.

Observation of Fast Striations Immediately after the Onset of Ionization

Eq. (III-13) predicts the existence of a medium in which striations are formed with variations of the density of ion pairs n in time and space as shown in Figs. 5 and 7 Chapter II. Although they were initially derived by pekarek for electron temperature θ_ν (Eq. II-29) to give a qualitative picture for the case of external perturbation of a homogeneous positive column, it is modified here to show how a similar picture drawn for ion pair

density n can justify the measurement in this work of what is shown to be the fast striations at the onset of ionization.

Such a conclusion was drawn on the basis of an experimental investigation [18] carried out under prebreakdown conditions in which under the same conditions as those of Pekarek's [26], similar results were obtained. However, the results reported here differ in nature from the above experimental study in two important respects:

(a) they are due to the phenomena leading to fast striations, rather than slow ones studied by the above investigators,

(b) they are valid even immediately after the onset of the ionization while the above results are obtained during the longer period before breakdown occurs.

The technique used in this work is entirely different and superior for the measurement made in comparison to the method used by the above workers. This technique will be explained in this chapter. For the purpose of comparing this work with the above investigations, the latter will be further discussed in this chapter as well as Chapter IV where the results are given.

The Measurement and Techniques

Eq. (III-13) is a good qualitative basis for the measurement made in this work, as will be discussed shortly. To use it for quantitative verification of any experimental observations on striations would need much further investigations of the dependences of the unmeasurable parameters α (and β for the case of slow processes) and B on some measurable quantities of the wave of stratification. However, a relation that gives a quantitative

basis for the observations made is derived in Chapter II (Eq. II-56) and a comparison of that theory with the results of this work will be given in Chapter IV.

The picture given by Eq. (III-13) with the approximate representation given in Fig. 5 shows how the velocity of the wave of stratification can be measured. A microwave Doppler reflectometer at X band region is used to make the velocity measurement. A brief description of the experimental apparatus, shown in Figs. 11 and 12, and the method of measurement are as follows:

The balancing arm of the Doppler reflectometer is connected to two attenuators and a phase shifter for the purpose of balancing the reflectometer with the other arm that looks, through a horn, into the discharge tube. The tube is ionized by means of a high voltage pulse with adjustable amplitude and pulse width. The ionization, when started, continues in the form of a wave of stratification with the velocity u giving rise to a reflection of the incident wave of frequency f_0. The reflected wave has a frequency $f_0 + \Delta f$, with Δf given by

$$\Delta f = 2f_0 \, u/c, \qquad \text{(III-14)}$$

where c is the velocity of light. The incident wave f_0 is mixed with the reflected wave $f_0 + \Delta f$ and the Doppler shift Δf can be observed on a spectrum analyser. Adjustments are made on the balancing arm of the reflectometer such that the most efficient (optimum) operation of the mixer is possible. This matter is further discussed in Appendix 1.

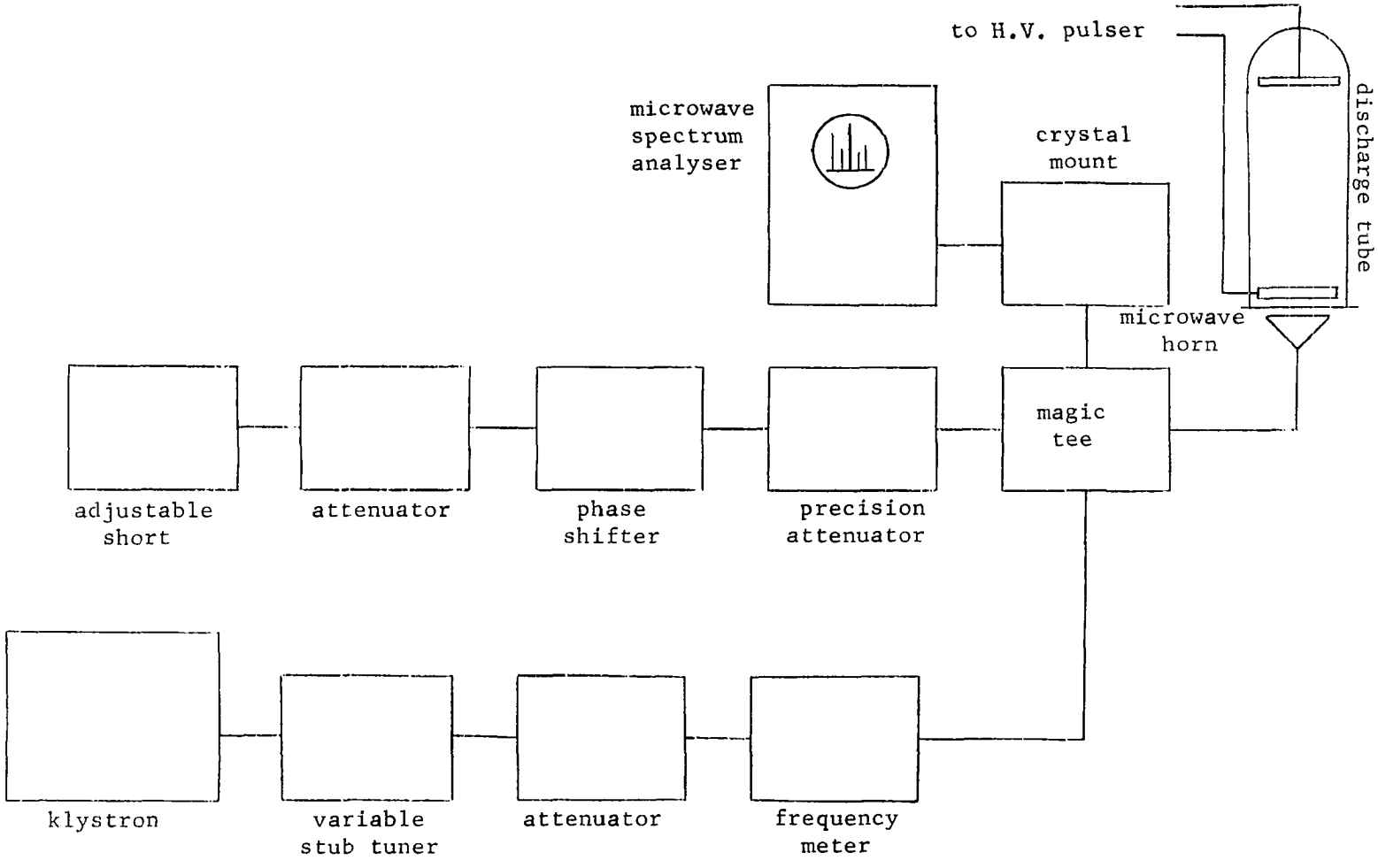

Fig. 11. Block diagram of the experimental apparatus.

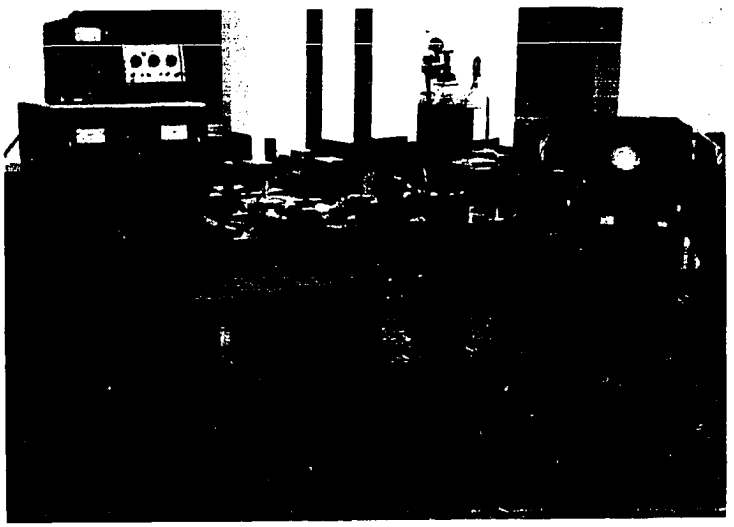

Fig. 12. Photograph of the experimental setup.

As previously discussed in Chapter II, the dotted line in Fig. 5 joining the center of each striation gives the velocity of the wave of stratification. The microwave horn in the Doppler reflectometer would make reflections of each of the striations as they are successively formed and travel along the tube. The abundant number of striations formed enables the horn to see a thick layer of plasma moving at an average velocity u which is observed on the spectrum analyser in the form of Doppler frequency spectra according to Eq. (III-14). This method has the advantage that it gives the velocity directly, while in the method in which photomultipliers and oscilloscope are used many measurements must be made before the plot of Fig. 5 is made, from which the velocity may be determined. In the method used by Neusel and Silver, who use a special camera with high space and time resolution, this velocity must be determined by interpretation of photographs similar to Fig. 5. Of course with these other methods the distance between striations, λ, can be measured easily. Without the improvement of the apparatus, perhaps the resolution of the analyser, the present method cannot be used to determine λ.

This method has proved successful in the Doppler measurement of the velocity of the wave of stratification. A number of tests have been carried out as evidence that the measurement is actually the intended measurement. These are discussed in Chapter IV where the results are reported. On the other hand, some techniques are proposed in that chapter for further improvement of this method and for more stable and more easily reproducible results.

Measurements Made on Slow Striations [13, 18, 20, 26]

As previously discussed in Chapter II, the self-excited striations may be caused by the repetition of the process of successive production of the wave of stratification. A simplified sketch of the apparatus used by Pekarek [25] for the production of the wave of stratification is shown in Fig. 13. An external perturbation is introduced at the point P, the cathode end of the positive column, which is homogeneous and unstriated. Photomultipliers are placed along the positive column and the light intensity can be observed through the photomultipliers on an oscillogram (not shown) in a similar manner as in Donahue and Dieke's experiment discussed in Chapter II. The

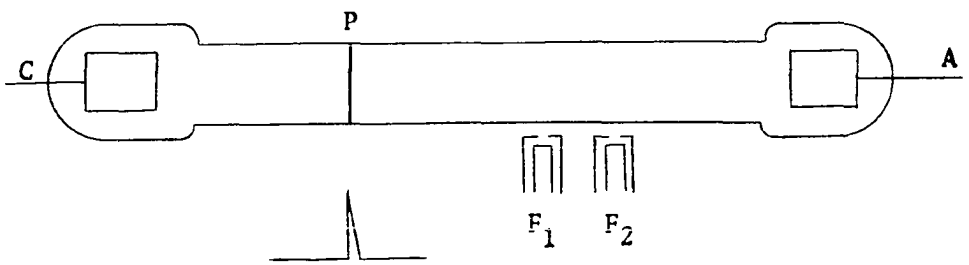

Fig. 13. Simplified sketch of Pekarek's apparatus for perturbation of the cathode end of the positive column.

change in light intensity as a function of time and space can then be plotted to obtain a picture similar to Fig. 5. Pekarek then concludes that a perturbation at the cathode end of the column in the same basic form as that artificially introduced above, produces a wave of stratification. This wave arrives at the anode region giving rise to oscillations of voltage and current of the discharge due to the motion of striations in the anode region. This process in turn gives rise to a further perturbation in the cathode region causing the above sequence of events to repeat all over.

Based on the above analysis and under similar conditions as those of the experimental study with the method of artifical perturbation of the positive column by Pekarek [26], Neusel and Silver [18] observed striations of the slower speed during prebreakdown. Instead of photomultipliers and oscilloscope technique used by Pekarek, they used a high speed image converter camera with high space-time resolution. They obtained pictures that closely resemble the picture of the wave of stratification shown in Fig. 5. From this picture they determined the velocity of propagation of the so called wave of stratification to be about 3.9×10^4 cm/sec. which is in close agreement with that obtained by Pekarek, namely 8.9×10^4 cm/sec. [26].

Independent of the above investigations, another worker [13,20] in an effort to measure the positive ion velocity at the onset of a gas discharge obtained a value of velocity averaging 4.1×10^4 cm/sec. which is very close to the above results. An analysis based on the assumptions of the work showed that the positive ion density is too low for any considerable reflection. (This problem is discussed in detail in Appendix 2). Thus, unless the ionization occurs in the form of strata, the amount of reflection will be insufficient for any observation. It can therefore be concluded that this

observation is actually the velocity of the slower striations observed by Neusel and Silver under prebreakdown conditions.

From the foregoing discussion of the work on the observation of slow striations and the present work on fast striations at the onset of ionization, it may be concluded that there may be a direct relationship between the striations formed at the onset, continued in a fairly similar manner during prebreakdown, and those observed when a homogeneous unstriated column is perturbed externally. It may thus be conceived that the striations in the positive column originate at the first moments when the gas starts to ionize. Thus, if the gas is allowed to continue to ionize until it glows, perhaps self-excited striations will be observed that result from the wave of stratification originated at the onset and continued to grow during prebreakdown. The formation of the striations at the onset may then be in the same manner as that observed by Pekarek in the positive column, namely by any aperiodic disturbance that may exist in the system initiating the wave of stratification.

This can be the subject of a new experimental and theoretical investigation. It is necessary for such investigation that, based on the observations made here of fast striations at the onset and those made of slow ones [13,18, 20,25,26], controlled disturbances be introduced immediately after the moment the gas starts to ionize, and the temporal growth of striations accurately observed up to and during the glow period. Then, based on the observations made, a theory may be developed to explain the observations. This matter is further discussed in Chapter IV where recommendations are made for further work on this subject.

Pekarek's Theory of Fast Striations [27]

It was discussed in Chapter II that a theory can be developed based on three basic phenomena occuring in a discharge: (a) the dependence of the rate of ionization on the electron temperature and hence on the electric field, (b) the production of space charges due to the different rates of diffusion of the electrons and ions, and (c) the creation of additional electric fields due to the creation of space charges.

Such analysis, it was explained, leads to a solution for the positive ion concentration in the form:

$$n_+(x,t) = \{[2/(-\pi a]^{1/2}/(-xt)^{1/4}\}\cos\,[a(-xt)^{1/2} - \pi/4], \tag{III-15}$$

and a relation for the velocity of striations

$$u = a^2\lambda^2/16\pi^2, \tag{III-16}$$

where the quantities are defined in Chapter II.

By substituting typical values in the expression for u, Pekarek [27] obtains a value of $u = 8.8\times10^6$ cm/sec. which is in close agreement with the velocity of fast striations obtained at the onset of ionization in the present work averaging about 3×10^7 cm/sec.

It is thus seen that the results obtained here is in agreement with the theory developed for the plasma of the positive column. The results will be reported in the form of the photographs of the Doppler spectra in Chapter IV. There, further discussion of the results will also be given.

CHAPTER IV

RESULTS, CONCLUSIONS, AND RECOMMENDATIONS

Results

It was shown in Chapter III that observations made of slow striations in prebreakdown [18] and in the case when the positive column is disturbed by an aperiodic perturbation [26] both lead to a picture similar to that shown in Fig. 5. The velocity u of the production of the wave of stratification has also been found to be of the same order of magnitude in both cases. It was seen further that an investigation [13] intended to determine the positive ion velocity in prebreakdown actually uses an independent method of measuring velocity of production of a slow wave of stratification. Such a velocity was seen to have a value in close agreement with those reported by the above researchers.

In the present work, the velocity of the production of the fast striations, formed at the onset of ionization, is found to agree with a theoretical analysis [27] made for the case when again an aperiodic perturbation is introduced in a homogeneous unstriated positive column.

The pictures shown in Figs. 14 are the Doppler frequency spectra Δf of the velocity u of the wave of stratification formed at the onset, where the relation between u and Δf is given by Eq. (III-14). The horn in the Doppler reflectometer set up of Fig. 11 will pick up reflections from each

layer of the wave of stratification (Fig. 5) as it is formed in succession as if a thick layer were moving with a velocity u.

Various lines in the spectra of Figs. 14 suggest that the velocities observed are not constant and in each case the average is taken. More lines are present than shown in each picture but the camera could not take all the lines since the spectrum shown on the analyser screen was not stable enough. Ideally, the Doppler frequency spectrum observed must be the Fourier analysis of a frequency modulated wave with the modulating function as the variations in the velocity so that a single line would have been observed for a constant velocity (Appendix 1).

It is seen from the photographs of Fig. 14c, for example, that the Doppler spectrum Δf averages about 20.1 MHz. This is equivalent to a velocity u of about 2.6×10^7 cm/sec. for the microwave frequency of about 11.30GHz used in the measurement. This value, as well as others obtained from other photographs, is in agreement with those found from theory [27] under typical discharge conditions.

The other spectra in Figs. 14 enable one to make a comparison of the results under different frequencies, gas pressures, electric field, r-f attenuator dials, and camera exposure times. The direction of variation of the velocity with such parameters and their significance will be discussed soon.

Discussion of Results

The reason for the instability of the spectrum is the fact that the initiation of ionization in the present technique is statistical. This is the case since overvoltage is used as an indirect means for the ionization. Under this condition the time lag between the application of the overvoltage and the appearance of initiatory electrons is statistical. This statistical time

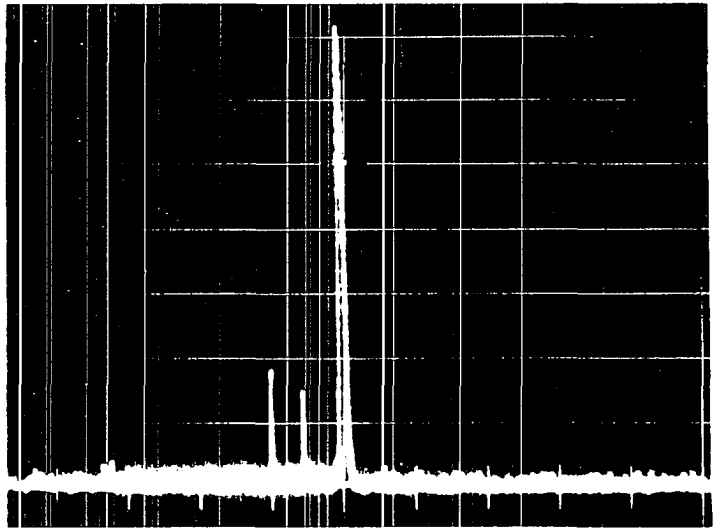

(a)

microwave frequency f_0=11.122 GHz
pressure = 0.250 Torr
r-f attenuator dial = 15
camera exposure time = 1/25 sec.
pulse amplitude = 1200 volts
Doppler frequency shift Δf = 19.2 MHz
velocity u (average) = 2.84×10^7 cm/sec.

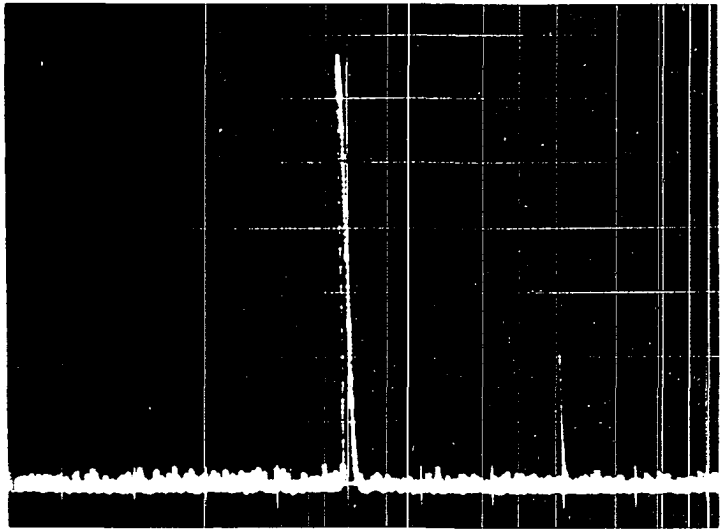

(b)

microwave frequency f_0 = 11.122 GHz
pressure = 0.170 Torr
r-f attenuator dial = 15
camera exposure time = 1/25 sec.
pulse amplitude = 1200 volts
Doppler frequency shift Δf = 21.0 MHz
velocity u (average) = 3.11×10^7 cm/sec.

Figs. 14a and b. Doppler spectra for a microwave frequency f_0 = 11.122 GHz.

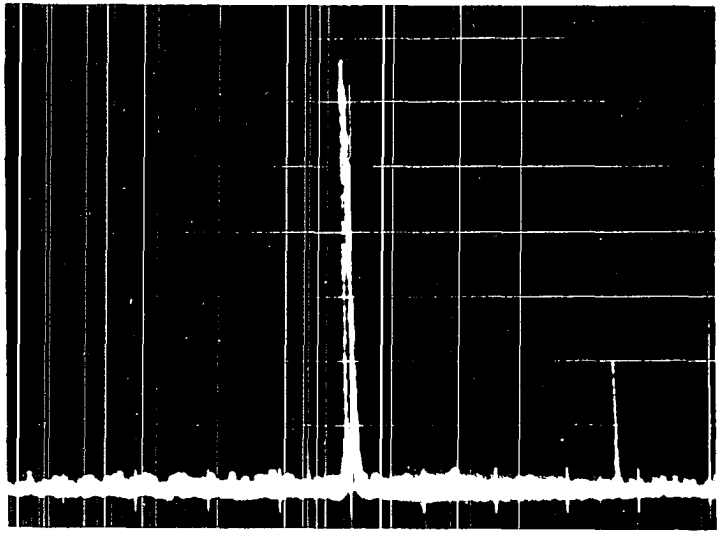

(c)

microwave frequency f_0 = 11.300 GHz
pressure = 0.180 Torr
r-f attenuator dial = 20
camera exposure time = 1/25 sec.
pulse amplitude = 1200 volts
Doppler frequency shift Δf = 20.1 MHz
velocity u (average) = 2.60×10^7 cm/sec.

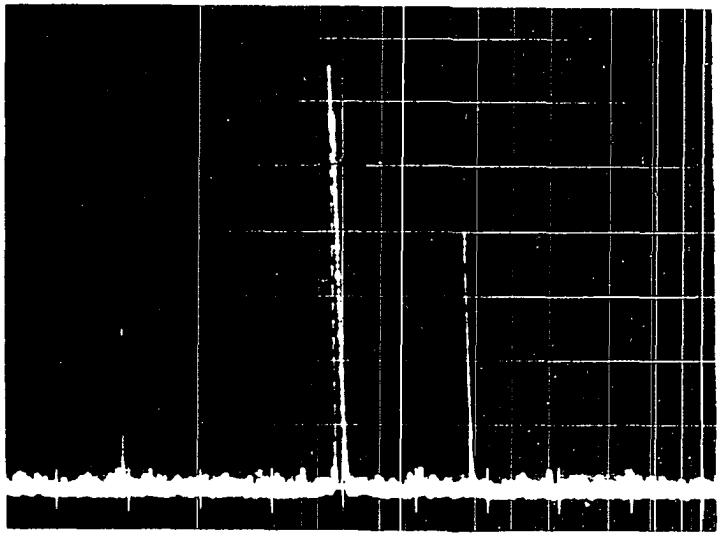

(d)

microwave frequency f_0 = 11.300 GHz
pressure = 0.190 Torr
r-f attenuator dial = 10
camera exposure time = 1/25 sec.
pulse amplitude = 1200 volts
Doppler frequency shift Δf = 20.5 MHz
velocity u (average) = 2.65×10^7 cm/sec.

Figs. 14c and d. Doppler spectra for a microwave frequency f_0 = 11.300 GHz.

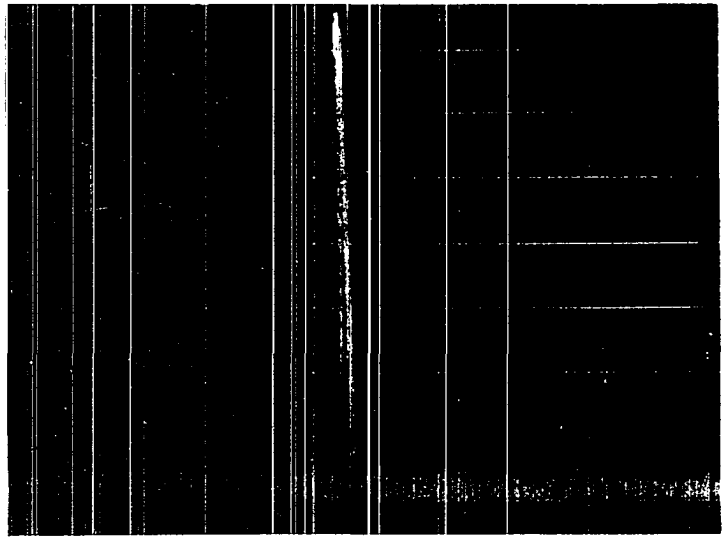

(e)

microwave frequency f_0 = 11.652 GHz
pressure = 0.180 Torr
r-f attenuator dial = 20
camera exposure time = 1/10 sec.
pulse amplitude = 1200 volts
Doppler frequency shift Δf = 22.0 MHz
velocity u (average) = 2.83×10^7 cm/sec.

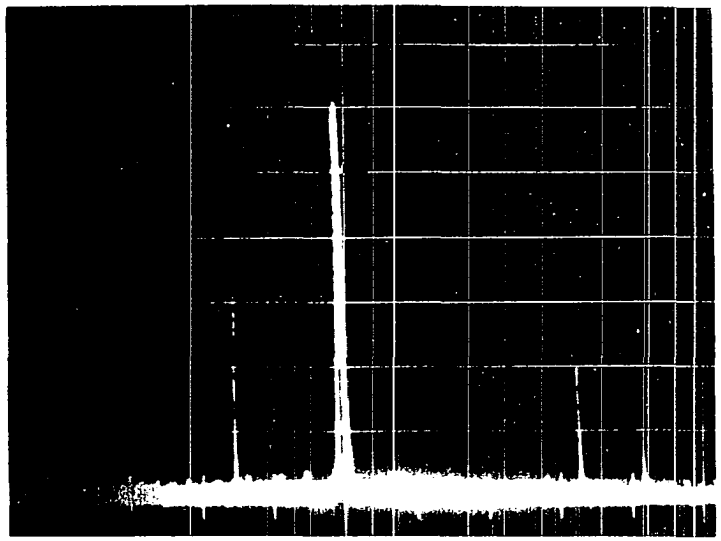

(f)

microwave frequency f_0 = 11.652 GHz
pressure = 0.190 Torr
r-f attenuator dial = 20
camera exposure time = 1/10 sec.
pulse amplitude = 1400 volts
Doppler frequency shift Δf = 23.2 MHz
velocity u (average) = 2.98×10^7 cm/sec.

Figs. 14e and f. Doppler spectra for a microwave frequency f_0 = 11.652 GHz.

lag is obtained from the relation [39]

$$n_t/n_0 = e^{-kt}, \qquad \text{(IV-1)}$$

where n_t is the number of trials which has not led to the appearance of initiatory electrons after time t, n_0 is the total number of trials, and k is a parameter which depends on the initial ionization and the fraction of voltage in excess of static breakdown value, $1/k = \tau_s$ is the statistical time lag.

This suggests that when the gas is ionized with the application of one voltage pulse and deionized after the disappearance of this pulse, the chances are that the time required for ionization of the gas by the next pulse is not the same as it was for the first pulse. Thus, a uniform and stable growth of ionization is not possible and this accounts for the instability of the observed spectra.

This difficulty of instability can be overcome if a method is used in which the cathode is irradiated by a rectangular pulse of ultraviolet light so that a pulse of electron current will be emitted from the cathode at a uniform rate for all pulses of the ultraviolet light. Then a high DC voltage can be applied across the discharge tube rather than a pulsed voltage to accelerate the ionizing electrons. This will be further discussed when recommendations are made for improvements and further investigations along the lines of this work.

Tests for Validating the Results

In order to make sure that the spectra observed were actually the Doppler frequency shift due to the motion of the ionized gas, some tests were carried

out with the results favoring the intended observation, as can be seen by comparing various photographs of the Doppler frequency spectra of Figs. 14. The description of the tests are as follows:

a) Dependence on the r-f signal. Since the Doppler frequency spectrum observed on the microwave spectrum analyser is the result of the mixing of the incident and reflected waves, its amplitude will depend on the amplitudes of both of the incident and reflected wave amplitudes (Appendix 1), and in general on the microwave signal amplitude. Thus, the attenuation of the signal in the balancing arm or horn arm of the reflectometer (Fig. 11) must attenuate the Doppler spectrum observed on the analyser. This was verified. A quick test could be carried out by attenuating the klystron attenuator and observing the decrease in the amplitude of the Doppler spectrum on the analyser screen.

b) Dependence on the gas pressure. Variation in pressure was made by opening a valve which sharply increased the pressure. Vacuum then gradually built up to a stable value. It was then observed, at higher pressures, that the spectrum disappeared from the screen of the analyser and as the pressure gradually decreased, the spectrum reappeared at a lower frequency range. The amplitude was then seen to gradually increase and the spectrum shifted to the right of the screen, an indication of a rise in frequency range.

The above observation is expected if the spectrum is due to the motion of the ionized gas in the tube. This is because the high pressure encountered at the initial variation of the gas pressure causes the mean free path to decrease to a point where almost no ionization occurs, thus no reflection from the discharge tube, and hence no Doppler shift. As the gas pressure

gradually decreases, the decrease in density gives rise to a larger mean free path, thus the beginning of ionization and the reappearance of the spectrum on the screen. Ionization increases causing higher ionized gas density and hence larger amount of reflection and the increase in amplitude of the Doppler spectrum. At the same time there is a rise in the frequency range of the spectrum as the pressure decreases because the resulting increase in mean free path permits greater acceleration of the charged particles before collisions.

c) The effect of voltage pulse amplitude. The increase in amplitude of the voltage pulse must increase the velocity of the charge carriers. Changes in voltage tappings that change the pulse amplitude were seen to change the frequency range observed. This is consistent with the picture given for the production of the wave of stratification described in Chapter II. In other words, the increase in the voltage causes an increase in the velocity of the initiatory electrons. This leads to the production of the space charge at a faster rate for a higher voltage. Thus, the weakening of the electric field due to the presence of the space charge is also faster causing the process of the production of the wave of stratification to occur at a higher rate (Chapter II: Fundamental Concepts in Pekarek's Theory).

Conclusions and Recommendations

The results obtained in this work suggest that a wave of stratification similar to that obtained by perturbing the positive column of a glow discharge exists immediately after the onset of ionization. This phenomenon is not previously observed as far as the search of the literature shows.

This observation along with those made of slow striations in prebreakdown [13,18] and by the method of aperiodic perturbation of a homogeneous positive

column suggest that there may be an interrelationship between the parameters of the wave of stratification observed at the onset, in prebreakdown, and during glow in the positive column. In this work, the existence of such wave of stratification at the onset and the agreement of the velocity of such a wave with the value predicted by a theory developed for the one occuring in a homogeneous positive column is shown. It is interesting to see if there is a relationship between the striations in various stages of a discharge. The following experimental procedure is believed to allow a systematic investigation of the growth of striations from the time ionization begins until the glow stage.

The experiment proposed should consist of introducing perturbations immediately after the beginning of ionization of the gas and observing the temporal growth of striations. The perturbation introduced may be delayed in subsequent trials by different time periods, and at a different point in the tube. Then observations can be made of light intensities at different points on oscilloscopes through photomultipliers for results other than at the onset. For measurement of velocity at the onset the method employed here is superior in that visible light is weak and photomultiplier techniques are not easy to use.

On the above basis various components of the experiment proposed with their functions is as follows:

a) Means to assure the uniformity of ionization. It was discussed earlier in this chapter that the irradiation of the cathode with the technique used here is provided from natural sources and ionization is thus initiated by the application of a high voltage pulse. The appearance of initiatory electrons is therefore statistical and as a result non-uniform.

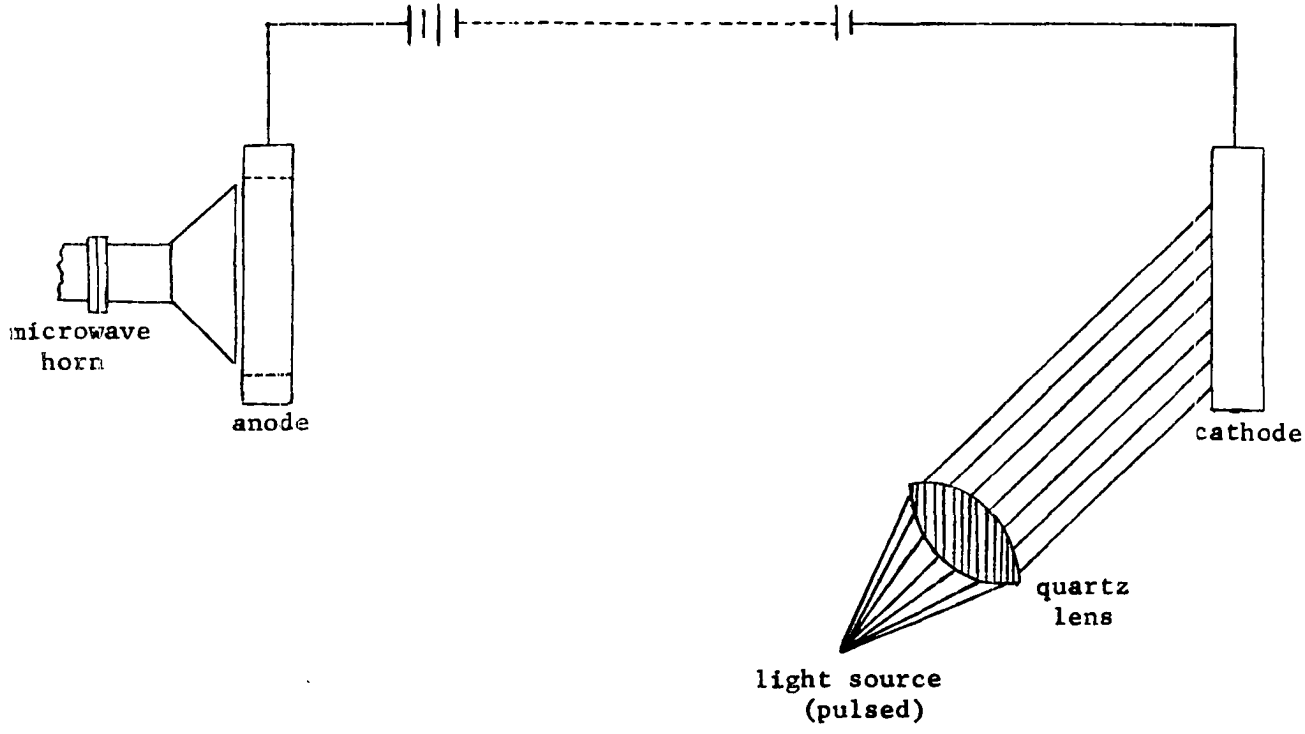

Fig. 15. Method of irradiating the cathode for a uniform electron emission.

In order to overcome this difficulty a pulsed sparking light source of variable duration can be used which can be impinged on the cathode at an angle through a quartz crystal as shown in Fig. 15. In this method then a high voltage DC supply is necessary to accelerate the uniform flow of electrons emitted from the cathode and to start ionizing the gas. Thus the relatively long period of statistical time lag will no longer exist and ionization will be uniform so that a stable Doppler spectrum can be observed. Furthermore, there will be better control over the formative time lag due to the fact that it will not be necessary to use voltages above the sparking voltage in order to initiate ionization [14,39], and thus a longer formative time lag can be maintained so that the prebreakdown period will be longer [7,14]. (It is known that the formative time lag varies in inverse relation with the voltage in excess of the spark voltage.) In this manner the problems encountered when observing the Doppler spectra, particularly the irreproducibility of the results partly due to a short time lag, can be overcome. Sometimes to reproduce the results reported takes many trials. This is due to the use of overvoltage as a means of ionization which causes a) the non-uniformity in ionization and b) a time lag relatively short and hard to control. Both of these contribute to irreproducibility of the results, besides the first being the reason for the instability of the Doppler spectrum.

Further details of this part will be given in Appendix III.

b) <u>External perturbation to investigate growth of striations</u>.

i) At the onset. Perturbations can be introduced in the form of sharp pulses of voltage, of small amplitude compared with the accelerating DC potential, and of frequency equal to that of the pulsed light source. The pulse will be used near the cathode end at a time after ionization has

started at the point of perturbation, but long before the ionization reaches the anode. Fig. 16 shows the time sequence of events for introducing the perturbation and Fig. 17 is a simple representation of the discharge tube, where the point of application of the external impulse is shown. The pulse width of the light source τ must be equal to the time when the ionization, started at the cathode by the emission of electrons, will reach the anode. The time t_1, when the external pulse is applied is to be taken slightly longer than the time required for ionization to reach from the cathode, to the distance d where the external impulse is applied to the grid-like electrode. This allows the wave of stratification, or a picture similar to it, to start almost immediately after the ionization begins.

If methods of observation of striations similar to that of the present work or those used by Donahue and Dieke [3], Pekarek [24], and Neusel and Silver [18] are used to measure the parameters of the striations, the above method should give improved data on the production of the wave of stratification at the onset of ionization investigated in this work. The method recommended thus assumes that the wave of stratification observed in this investigation is the result of disturbances inherent in the system used here. It may, for example, be due to fluctuations in the flat top of the high voltage pulse, statistical fluctuations in ionization, or any other similar reason. In the proposed method of course, the ripple in the accelerating DC power supply must be small compared with the perturbation impulse introduced and the intensity of the pulsed light source must be such that it would not cause fluctuation in ionization larger than that caused by the perturbation impulse. When such conditions are met, a controllable perturbation can be introduced and observations similar to those of the present

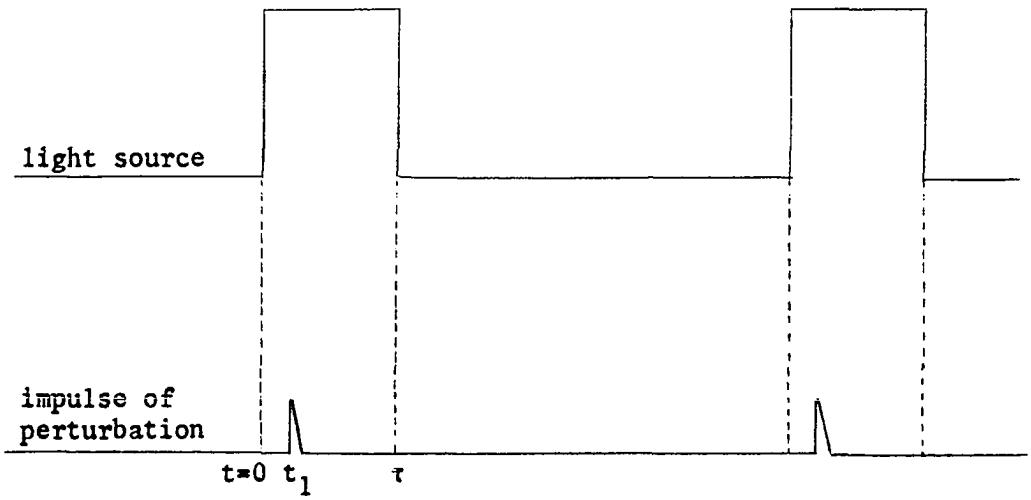

Fig. 16. Relative sequence of the application of external perturbation.

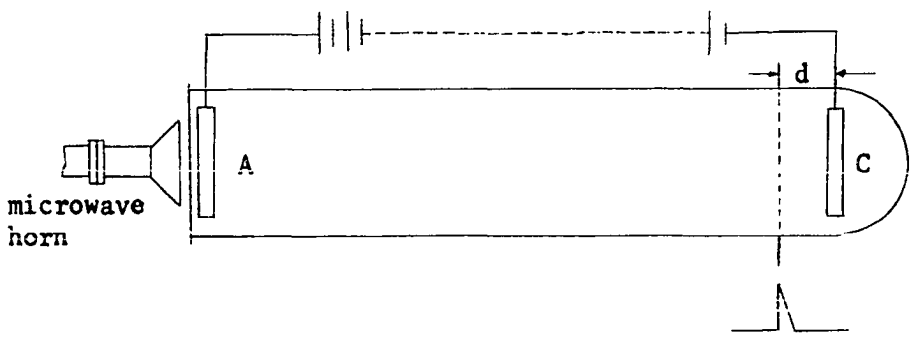

Fig. 17. Method and point of perturbation of the discharge.

work be repeated more systematically with more easily reproducible results.

A discussion is necessary here about difficulty in reproducing the present results. It was mentioned in Chapter II that long waiting periods were necessary for reproducing the results under steady-state striation conditions. It was also mentioned that to avoid the complications in steady state striations, Pekarek used transient methods fully discussed in that chapter. The method used in this investigation does not have the complications of the steady-state striations because it is confined to the period from the beginning of the ionization until the wave of stratification produced travels the length of the tube. Thus the reason for irreproducibility of the results in this work is the waiting period for a suitable disturbance to occur. The disturbance must be of such magnitude as to cause enough inelastic collisions to give rise to the processes in Chain I of the phenomena, discussed in Chapter II, which are the cause of fast striations. (It has been fully discussed in Chapter II that in Chain I only one time constant α is involved while in Chain II there exists also another time constant β in addition to α, which when sufficiently effective, will slow down the production of the wave of stratification).

With the method proposed above, a waiting period for the occurence of a disturbance for the production of the fast wave of stratification is not necessary. The phenomena leading to such a wave can be implemented by using the external perturbation impulse of large enough amplitude, thus making the results easy to reproduce.

ii) During prebreakdown. In a manner similar to that discussed above, perturbations can be introduced in the tube at various instances before

breakdown of the gas and developments following the perturbation observed with similar techniques. In this manner the effect of any disturbances occuring in prebreakdown can be investigated and their effect compared with the nature of the striations in the positive column.

In addition to introducing the perturbation at different times during the ionization growth, the point where it is introduced may also have an effect on the growth of striations. This is particularly true after the breakdown when a steady-state glow is maintained. Thus the experiment intended to study the growth of striations will be more complete if perturbations are introduced at various points in the tube both during prebreakdown as well as under steady state glow conditions. Although Pekarek has already performed experiments by perturbation of the positive column, he always perturbed the cathode side of the positive column. There seems no reason why a disturbance at other points in the tube would not lead to the processes leading to the production of the wave of stratification or a similar picture.

The experiments proposed above obviously would be very extensive but are believed to be useful and enlightening in that they reveal more of the phenomena of the existence of striations.

The theoretical analysis of the complex problem posed above may involve the superposition of the perturbation on the temporal growth of ionization [16,27,39] for the case of onset and prebreakdown. For the steady state glow, in the positive column this will involve processes similar to those investigated by Pekarek which can thus be analysed in a similar manner. For perturbations introduced at points other than the positive column, the processes [39] leading to the presence of dark and glow regions will be slightly disturbed based on the effect of the perturbation introduced on such processes.

It is thus seen that for every phase in the development of the ionization, the analysis is different. Nevertheless, for a problem of such analytical complexity, it is best that an experimental investigation be made first and the analysis be carried out to see if verification of the results is possible.

BIBLIOGRAPHY

[1] Beams, J.W., A.R. Kuhlthau, A.C. Lapsley, J.H. McQueen, L.B. Snoddy, and W.D. Whitehead, Jr., "Spark Light Source of Short Duration", Journal of Optical Society of America, 37 (1947), pp. 868-70.

[2] Cobine, J.D., Gaseous Conductors, Theory and Engineering Applications, Dover Publications, New York, 1958.

[3] Donahue, T. and G.H. Dieke, "Oscillatory Phenomena in Direct Current Glow Discharges," Physical Review, 81 (1951), pp. 248-261.

[4] Druyvestyn, M.J. and F.M. Penning, "The Mechanism of Electrical Discharges in Gases at Low Pressure," Reviews of Modern Physics, 12 (1940), pp. 87-174.

[5] Francis, G., The Glow Discharge at Low Pressure, Handbuch der Physik, XXII, Springer-Verlag, Berlin, 1956.

[6] Francis, G., Ionization Phenomena in Gases, Chapter 7, Academic Press, New York, 1960.

[7] Fisher, L.J., "Formative Time Lags of Spark Breakdown", Report of the International Symposium on the Electrical Discharges in Gases, Delft, Netherlands, April 1955.

[8] Ginzton, Edward L., Microwave Measurements, Chapter 5, McGraw Hill Book Company, New York, 1957.

[9] Hilderbrand, Francis B., Advanced Calculus for Applications, Chapter 3, Prentice Hall, Englewood Cliffs, New Jersey, 1962.

[10] Hornbeck, John A., "Microsecond Transient Currents in the Pulsed Townsend Discharge," Physical Review, 83 (1951), pp. 374-379.

[11] Hornbeck, John A., "The Drift Velocities of Molecular and Atomic Ions in Helium, Neon, and Argon," Physical Review, 84 (1951), pp. 615-620.

[12] Johnson, J.B., "Thermal Agitation of Electricity in Conductors," Physical Review, 32 (1928) pp. 97-101.

[13] Ling, H., The Investigation of Ion Velocity in Electrical Prebreakdown Using Microwave Doppler Reflectometer Technique Ph.D. Dissertation, University of Oklahoma; Norman, Oklahoma, 1965.

[14] Llewellyn Jones, F., Ionization and Breakdown in Gases, John Wiley and Sons, New York, 1957.

[15] Llewellyn Jones, F., Ionization Growth and Breakdown, Handbuch der Physik, XXII, Springer-Verlag, Berlin, 1956.

[16] Loeb, Leonard B., Basic Processes of Gaseous Electronics, University of California Press, Berkeley, 1955.

[17] Mc Daniel, Earl W., Collision Phenomena in Ionized Gases, John Wiley and Sons, 1964.

[18] Neusel, T.H., and M. Silver, "Striation Production during Electrical Breakdown in Hydrogen," Journal of Applied Physics, 36 (1965), pp. 1507-9.

[19] Newton, Robert R., "Transients in Townsend Discharge," Physical Review, 73 (1948) pp. 570-83.

[20] Palmer, J.D., and H. Ling, "The Use of Doppler Shift for Direct Measurement of Ion Velocity in Gas Discharge Onset," Proceedings of Institute of Electrical and Electronics Engineers, 53 (1965), p. 661.

[21] Pekarek, L., "Oscillation Phenomena in Glow Discharges in Neon," Czechoslovak Journal of Physics, 4 (1954), pp. 221-32.

[22] Pekarek, L., and Oto Stirand, "The Energetic Conditions in a Striated Electric Discharge," Czechoslovak Journal of Physics, 6 (1956), pp. 365-75.

[23] Pekarek, L., "A Theory of Successive Production of Moving Striations in the Plasma of Inert Gases," Czechoslovak Journal of Physics, 7 (1957), pp. 533-56.

[24] Pekarek, L., "Theory of Moving Striations," Physical Review, 108 (1957), pp. 1371-72.

[25] Pekarek, L., "Local Excitation of the Wave of Stratification in the Positive Column of an Electric Discharge," Czechoslovak Journal of Physics, 8(1958), pp. 498-9.

[26] Pekarek, L., "The Successive Production of Striations in a Glow Discharge in Hydrogen," Czechoslovak Journal of Physics, 8 (1958), pp. 699-704.

[27] Pekarek, L., and V. Krejci, "The Physical Nature of the Production of Moving Striations in a D-C Discharge Plasma," Czechoslovak Journal of Physics, B11 (1961), pp. 729-42.

[28] Pekarek, L., V. Krejci, and O. Stirand, "Motion of Striations in an Inert Gas-Hydrogen Mixture," Czechoslovak Journal of Physics, B13 (1963), pp. 243-45.

[29] Pound, R.V., Microwave Mixers, Radiation Laboratory Series, 16, McGraw Hill Book Company, New York, 1948.

[30] Ratcliffe, J.A., The Magneto-Ionic Theory and its Applications to the Ionosphere, Cambridge at the University Press, 1959.

[31] Reich, Herbert, J., Philip F. Ordung, Herbert L. Krauss, and John G. Shalnick, Microwave Theory and Techniques, D. Van Nostrand Company, Princeton, New Jersey, 1953.

[32] Robertson, Harry S., "Moving Striations in Direct Current Glow Discharges," Physical Review, 105 (1957) pp. 368-77.

[33] Sucher, Max, and Jerome Fox, Handbook of Microwave Measurements, Vol I, Polytechnic Press of the Polytechnic Institute of Brooklyn, New York, 1963.

[34] Sucher, Max, and Jerome Fox, Handbook of Microwave Measurements, Vol. III, Polytechnic Press of the Polytechnic Institute of Brooklyn, New York, 1963.

[35] Thomson, J.J., and G.P. Thomson, Conduction of Electricity through Gases, Cambridge University Press, London, 1933.

[36] Torrey, Henry C., and Charles A. Whitmer, Crystal Rectifiers, Radiation Laboratory Series, 15, McGraw Hill Book Company, New York, 1948.

[37] Van der Pol, B., and H. Bremmer, Operational Calculus, Cambridge University Press, Cambridge, England, 1955.

[38] Van Voorhis, S.N., Microwave Receivers, Radiation Laboratory Series, 23, McGraw Hill Book Company, New York, 1948.

[39] von Engel, A., Ionized Gases, Oxford at the Clarendon Press, 1955.

[40] Watanabe, M.S. and N.L. Oleson, "Travelling Density Waves in Positive Columns," Physical Review, 99 (1955), pp. 1701-4.

[41] Whitmer, R.F., "Microwave Studies of the Electron Loss Processes in Gaseous Discharges," Physical Review, 104 (1956) pp. 572-81.

APPENDIX 1

MEASUREMENT OF STRIATION VELOCITY USING MICROWAVE RECEIVER TECHNIQUES

General Considerations on Doppler Frequency Measurement

In this work, frequency conversion techniques are used to observe the Doppler shift caused by the "motion" observable due to the successive production of the wave of stratification at the onset of ionization, discussed in the context. However, the frequency conversion in this work is not exactly similar to the conventional methods.

In an ordinary superheterodyne receiver used in communication systems, frequency conversion is accomplished through the combined use of a local oscillator and a mixer. The local oscillator is simply a continuous-wave oscillator operating at a frequency somewhat different from that to which the receiver is to be sensitive. In the mixer, a superposition of the local oscillator wave and the input signal takes place. A beat, or heterodyne, frequency equal to the difference between the two waves exists at the output of the mixer in the form of a current or voltage.

In the above arrangement the local oscillator is a source completely independent of the signal. However, in the present work a microwave signal shifts in frequency by an amount that is proportional to the velocity of the "moving" layer. These incident and reflected signals are sampled and used as the inputs to the microwave mixer.

The microwave set up that can be used for sampling the incident and reflected waves, is an ordinary reflectometer usually used for impedance measurements [8, 33]. A simplified diagram of such a set up is shown in Fig. 18. The incident and reflected waves are sampled through two directional couplers and taken into a crystal mixer. The klystron oscillator in this experiment is operated on a continuous-wave (CW) mode so that a single frequency component exists in both the incident and reflected waves. In the superheterodyne receivers ordinarily used however, the input to as well as the output from the mixer are modulated. The advantages of the mode presently used will be discussed shortly.

Now assume a square law crystal and let A be the amplitude for the incident and B for the reflected wave; it can then be easily shown that the components at the output of the mixer will have frequencies $2f$, $2(f+\Delta f)$, $2f+\Delta f$, Δf, and zero (dc), where Δf is the frequency of the incident microwave signal and Δf the desired Doppler frequency shift. The amplitude of the Doppler shift Δf can be shown to be AB. The frequency Δf, obtainable from Eq. (III-14), is very small in comparison with the other components for the velocities of motion encountered in this measurement, as can be seen from the results reported in Chapter IV. Thus the frequency of this component is much smaller than the the other components so that no filtering is needed for the separation of Δf from the other components.

The signal flow in the reflectometer used in Fig. 18 can be easily visualized and the analysis is ideally as discussed above. However, errors result due to poor directivity of the directional couplers sampling the incident and reflected signals. Furthermore, even with a directional coupler of the lowest attenuation some valuable reflected signal will be lost.

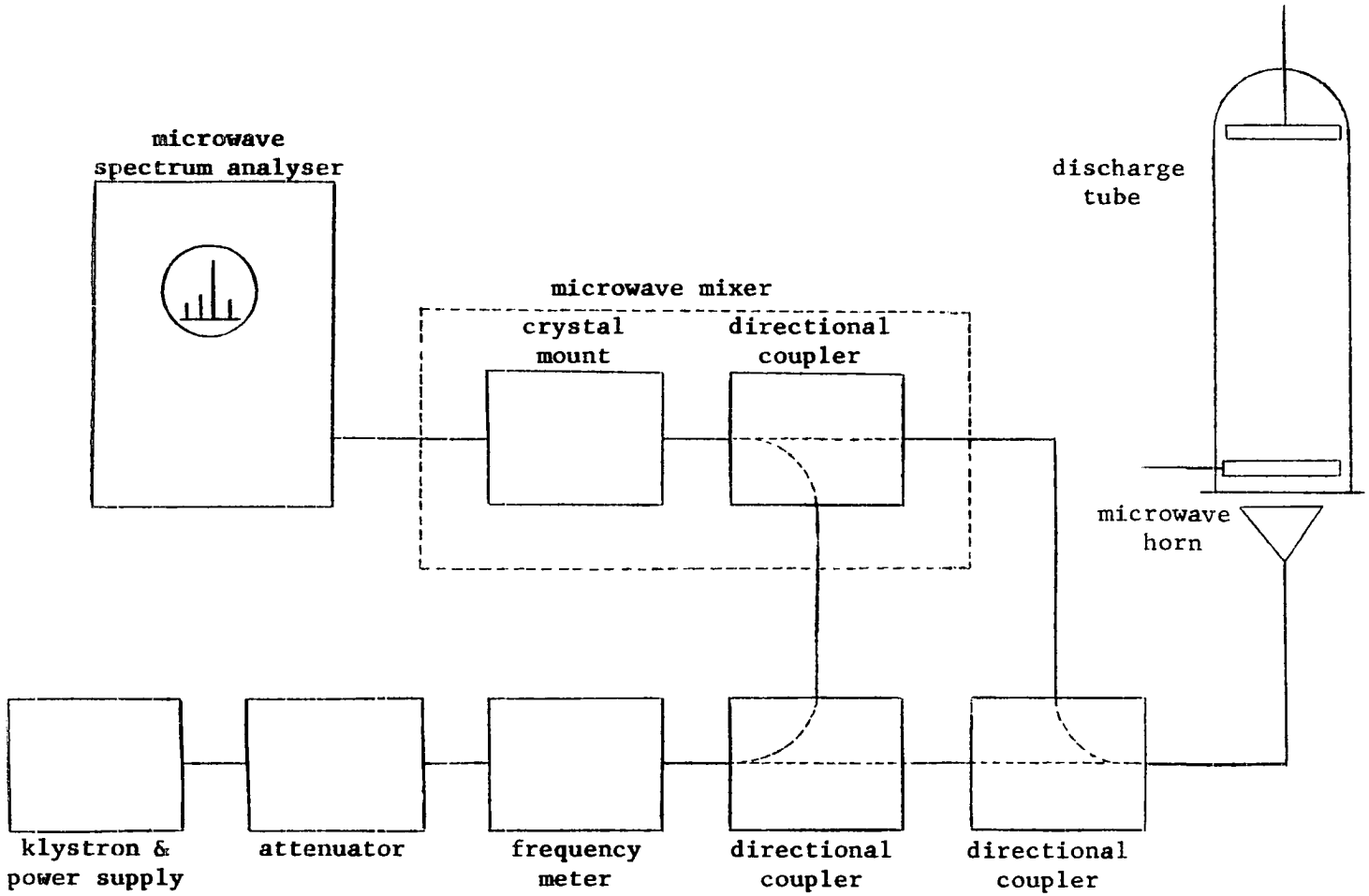

Fig. 18. Ordinary microwave reflectometer.

Besides, some reflection losses will be caused in the paths from the couplers to the mixer. Such errors can be avoided by using a Doppler reflectometer. It will be shown in the next section that when the Doppler reflectometer is used, as far as frequency components are concerned, the mixer will be supplied with similar inputs and will thus give similar outputs as the ordinary reflectometer without introducing the losses present in the ordinary reflectometer

Doppler Reflectometer - A Signal Flow Analysis

The Doppler reflectometer, already briefly discussed in Chapter III and shown in Fig. 11, is the one actually used for the measurement of the velocity of striations. In this case, however, adjustments are made on the main arms of the magic tee to which the balancing arm and the horn arm of the reflectometer are connected, so that at the E plane arm of the magic tee, a sample of both the reflected and incident waves are present. Thus the mixer may be connected to this arm instead of using the weakened samples brought from the directional couplers as in the ordinary reflectometer of Fig. 18.

In the Doppler reflectometer of Fig. 11, the signal from the klystron propagates in the H plane arm of the magic tee and is divided between the two main arms. One of these arms is connected to the horn facing the discharge tube and the other is the balancing arm that is terminated with a short. Assuming as before that the incident and reflected signals in the two arms have amplitudes A and B respectively, the general expression for the output V at the E plane arm is given by the equation [31,41]

$$V = [A^2 + B^2 + 2AB \cos (\phi_A - \phi_B)]^{1/2}, \qquad (1-1)$$

where $(\phi_A - \phi_B)$ is the phase difference between the two arms with amplitudes A and B respectively.

Adjustments can be made on the balancing arm by variation of attenuation and phase shift such that the phase difference $\phi_A - \phi_B$ between the two arms is zero so that the output at the E plane will be A+B according to Eq. (1-1). This will then serve as the input to the mixer in the same way as if the incident and reflected waves were sampled by directional couplers without the presence of the losses inherent in using directional couplers, as previously mentioned.

Microwave Receivers - Their Figures of Merit

For this investigation a superheterodyne microwave receiver is set up in which frequency conversion is performed by means of a crystal mixer since the crystal rectifier is the most effective mixer element at microwave frequencies. The microwave receiver used here differs from the conventional ones in that the balancing arm of the Doppler reflectometer functions as a local oscillator. Before going into the discussion of optimum operation of the mixer, it is necessary to consider the limitations imposed on a microwave receiver and its various components.

A fundamental limitation on the sensitivity of any radio receiver, as is well known, arises from sources of noise in the circuit elements or from external sources [38]. Even in a theoretically perfect receiver, namely one containing no sources of noise within itself, the minimum detectable signal will still be limited by the Johnson noise in the input impedance.

It is the generally accepted practice to express the ability of a microwave receiver to detect weak signals in terms of its noise figure which is a

quantitative indication of just how much worse the actual receiver is than an idealized one. In an actual microwave receiver, employing a crystal mixer, such as the one devised for this investigation, the output noise will consist of the noise originating in the i-f amplifier - the spectrum analyser in this case - plus that originating in the mixer. In the mixer itself the crystal, driven by a local oscillator, in general generates more i-f noise than a resistor with the same i-f impedance [36]. This is one of the properties that is of importance in the mixer application.

Even if the crystal should generate only Johnson noise (which is approximately the case for occasional units), an additional limitation arises from the fact that in the frequency conversion process not all the available power in the r-f signal is converted into power at intermediate frequency. This conversion loss is therefore a second crystal property affecting its mixer performance.

Before giving discussions that lead to the important relationship between noise figure, conversion loss, and noise temperature, it seems necessary to discuss the general principles underlying the operation of a crystal mixer.

The Crystal Converter General Behavior [29]

The crystal rectifier, when used as a frequency converter, is operated under conditions rather different from those in the low-level detector application. For this reason, an entirely different set of parameters are used for the evaluation of the quality of a unit intended for use as a frequency converter. This can be seen from a simplified consideration of the mechanism of rectification based on the d-c characteristic of Fig. 19. Although an analysis based upon the d-c characteristic gives a poor picture of the

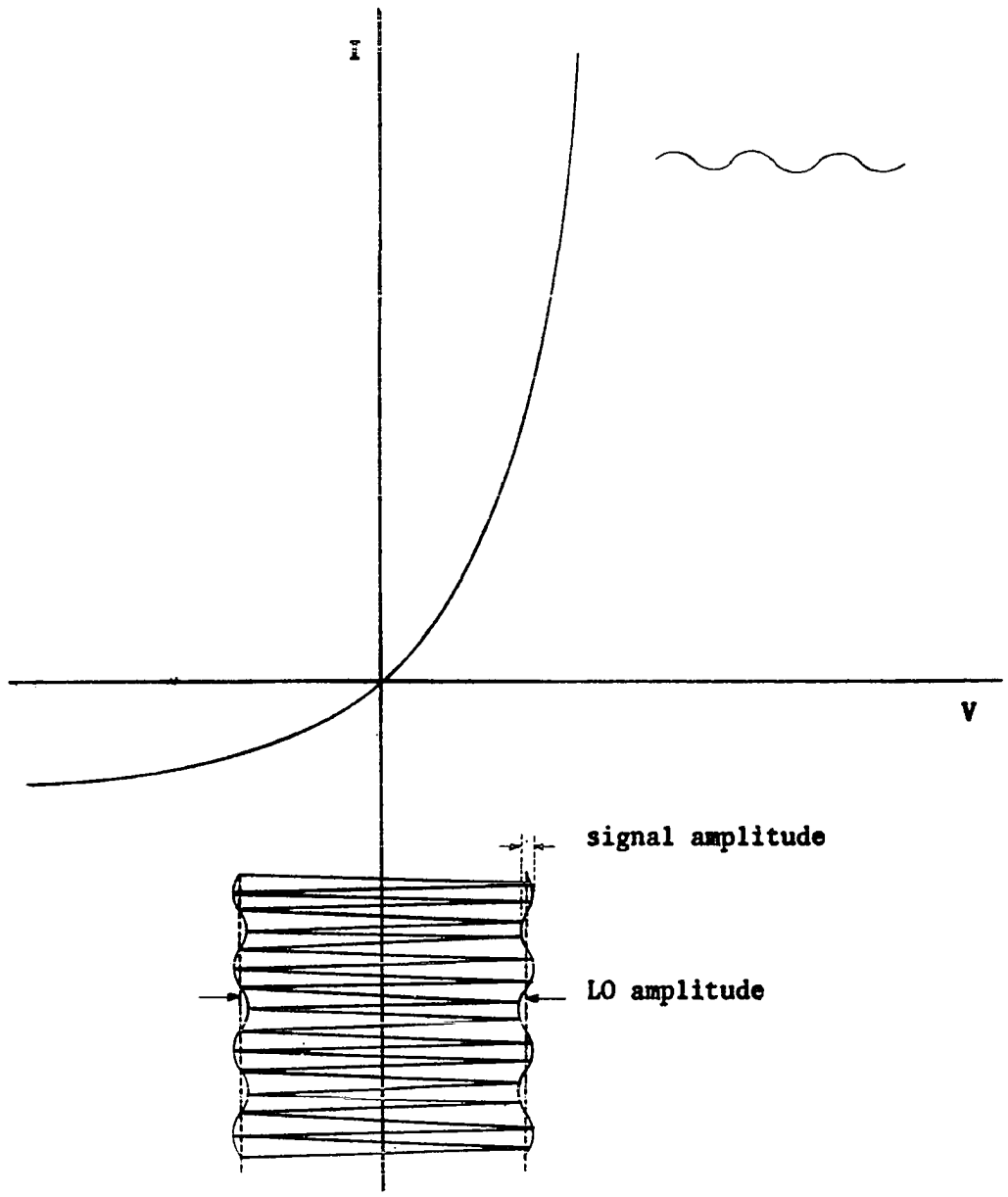

Fig. 19. Graphical illustration of frequency conversion on the basis of d-c characteristic of crystal.

microwave behavior of the contact as a frequency converter, because of the barrier capacitance, it does serve a qualitative description.

In Fig. 19, a typical characteristic is shown. In addition there is shown, as a function of time along the negative ordinate axis, a voltage corresponding to the superposition of the local oscillator voltage upon a small signal voltage. The output terminals of a crystal mixer are so arranged that no microwave frequency component of the current in the crystal will appear at them. The output terminals carry only the direct current and the beat frequency components, as indicated by the curve representing the current as a function of time plotted along the right-hand part of the horizontal axis.

The magnitude of the beat-frequency component in this current is related to the efficiency of the device as a frequency converter or its inverse, the conversion loss. From the diagram it is evident that the magnitude of this beat frequency component depends primarily upon the ratio of the d-c characteristic at the negative peak and at the positive peak of the local oscillator voltage. It is apparent that the curvature of the characteristic in the vicinity of the origin is of little direct importance compared with the ratio of what might be called the differential impedances at two points symmetrically chosen at some distance on either side of the axis. From this consideration, it would be expected that the crystal rectifiers that make the best detectors do not necessarily make the best units for use as frequency converters. Care was therefore exercised in the experiment to choose a crystal suitable for a frequency converter.

Another significant relationship is the dependence of the conversion loss on the magnitude of the local oscillator voltage applied. If the signal

is kept small compared with that of the local oscillator but of constant magnitude, and the amplitude of the local oscillator voltage is varied, the magnitude of the modulation component in the linear superposition of the two voltages remains constant. Because of the curvature of the d-c characteristic, particularly on the positive side of the zero voltage, the ratio of the differential impedances on the two sides diminished with decreasing local oscillator voltage and, as a result, the conversion loss of the device should be more with small local oscillator amplitudes than with large amplitudes. This accounts for the shape of the curve of conversion loss versus local oscillator current shown in Fig. 20.

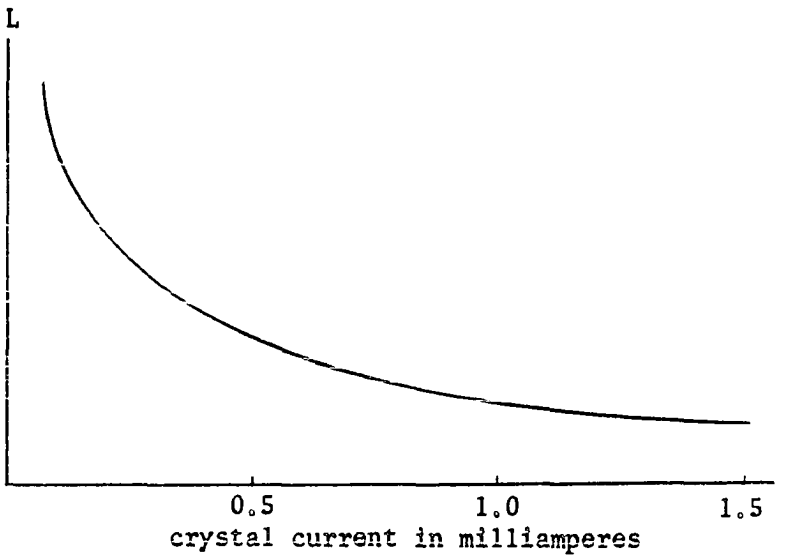

Fig. 20. Typical curve for conversion loss L vs. local oscillator drive.

Relationships will be given for the dependence of the crystal noise temperature and receiver noise figure on the local oscillator current which together with the dependence of receiver noise figure on conversion loss and crystal noise temperature will determine the conditions for the optimum operation of the converter. This matter will be discussed in the following sections. Procedure followed in the experiment for maintaining optimum operation will then be outlined.

Dependence of Receiver Noise Figure on Crystal Noise Temperature and Conversion Loss

For this derivation a four-terminal network will be considered that is connected to a signal generator and an output circuit as shown in Fig. 21.

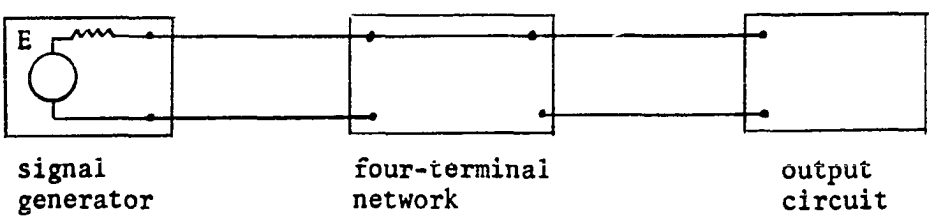

Fig. 21. Block diagram for the analysis of the network noise figure.

The input and output impedances of the network may have reactive components and may or may not be matched to the generator and output circuit.

Gain of the Network

The signal generator may be regarded as a voltage source E in series with an impedance R+jX. To get the maximum power into a load, the load should have an impedance R-jX. This maximum power is by definition the available power from the signal generator, and is given by the expression

$$S = E^2/4R. \tag{1-2}$$

Similarly, the output terminals of the network can be treated as a new source of signal, having an available power output, which will be called S. The power gain G of the network is defined by the relationship

$$G = S_0/S. \tag{1-3}$$

The gain is by definition independent of the impedance presented to the network by the output circuit but is a function of the generator impedance. It is apparent that for some particular generator impedance the power gain will be a maximum, G_m.

Noise Figure

For making measurements of noise power, a practical standard of comparison is the Johnson noise generated in a resistor. The available noise power from a resistor into a "cold", or noiseless, load in an incremental band of frequency df is given by the expression [12]

$$dN = kTdf, \tag{1-4}$$

where k is Boltzmann's constant, N is the available noise power, and T is the absolute temperature.

In so far as noise considerations are concerned, a perfect network is one where there are no noise sources within the network itself. Actually, such noise sources exist; in such a case the ratio dN_0/S_0 of available output noise power to available input signal power is greater than the ratio dN/S of available input noise power to available input signal power. The noise figure F of the network is then defined as

$$dN_0/S_0 = F(kT_0df)/S \tag{1-5}$$

in which kT_0df is the available input noise power from a resistor. From Eqs. (1-3) and (1-5) there is obtained

$$dN_0 = FGkT_0df. \tag{1-6}$$

The noise output, noise figure, and the gain are alike in that all are functions of the impedance of the generator. The noise figure is a minimum for some particular value of generator impedance, which in general is not the same as that giving maximum gain.

Effective Noise Figure

The total available noise output of a practical network that has a finite bandwidth is given by

$$N_0 = kT_0 \int_0^\infty FGdf. \tag{1-7}$$

Eq. (1-5) can now be rewritten in the form

$$dN_0/dN = FG. \tag{1-8}$$

The effective noise figure F' is now defined as

$$F' = N_0/N_0', \tag{1-9}$$

where N_0' is the available output noise power if F were unity at all frequencies, that is

$$N_0' = kT_0 \int_0^\infty G df. \tag{1-10}$$

In other words, N_0' is the noise that would be delivered to the output load if there were no noise sources within the network.

The effective noise figure F' is then given by the relation

$$F' = N_0/N_0' = \int_0^\infty FG df / \int_0^\infty G df. \tag{1-11}$$

The effective, or noise, bandwidth B of the network can now be defined as

$$B = \int_0^\infty G df/G_{max}, \tag{1-12}$$

where G_{max} is the maximum gain versus frequency characteristic.

Introducing Eq. (1-12) into (1-11), the following expression is obtained for the effective noise figure:

$$F' = N_0/kT_0BG_{max} \,. \tag{1-13}$$

This equation gives F' in terms of measurable quantities.

Noise Figure of Two Networks in Cascade

The noise figure of two networks in cascade can now be obtained in terms of the properties of the two networks.

Applying Eq. (1-4) to the two networks as a whole, the noise output in the incremental frequency band df is obtained:

$$dN_{0(1+2)} = F_{1+2}\, G_{1+2}\, kT_0 df, \tag{1-14}$$

where the subscript $(1+2)$ indicates that the quantity applies to the over-all network. From the relation $G_{1+2} = G_1\, G_2$ for the over-all gain, it follows that

$$dN_{0(1+2)} = F_{1+2}\, G_1 G_2 kT_0 df. \tag{1-15}$$

Similarly, Eq. (1-4), applied to network 1, gives

$$dN_{01} = F_1\, G_1\, kT_0 df. \tag{1-16}$$

The part of the output noise from network 2, originating in the signal generator and network 1 is

$$dN'_{0(1+2)} = dN_{01}\, G_2 = F_1 G_1 G_2\, kT_0 df. \tag{1-17}$$

The part of the output noise from network 2 originating within network 2 is

$$dN''_{0(1+2)} = F_2 G_2 kT_0 df - G_2 kT_0 df. \tag{1-18}$$

The second term of the right-hand member of Eq. (1-18) is subtracted in order not to include for a second time the Johnson noise from the output resistance of network 1.

The addition of Eqs. (1-17) and (1-18) gives for the total output power the relation

$$\begin{aligned} dN_{0(1+2)} &= dN'_{0(1+2)} + dN''_{0(1+2)} \\ &= F_1 G_1 G_2 kT_0 df + F_2 G_2 kT_0 df - G_2 kT_0 df. \end{aligned} \tag{1-19}$$

Equating the right-hand members of Eqs. (1-15) and (1-19), there is obtained

$$F_{1+2} = F_1 + (F_2 - 1)/G_1. \tag{1-20}$$

Using Eq. (1-20) and the relation $G_{1+2} = G_1 G_2$, the effective noise figure is obtained:

$$F'_{(1+2)} = \int_0^\infty [G_1 G_2 F_1 + G_2 (F_2 - 1)]\, df / \int_0^\infty G_1 G_2 df. \tag{1-21}$$

If network 2 has a small bandwidth compared with network 1, G_1 and F_1 may be considered constant over the range of integration; in this case Eq. (1-21) reduced to

$$F'_{1+2} = F_1 + (F'_2 - 1)/G_1. \qquad (1\text{-}22)$$

It must be emphasized that F_2' is a function of the output impedance of network 1, which is considered as a generator for network 2. In applications of this equation, the measurement of F_2' must be made with a signal generator having the same terminal impedance as the output impedance of network 1.

The above derivations are made for any general case, but they are applicable to microwave receiver systems such as the one set up for the present investigation. Eq. (1-22), for example, is of particular interest in the evaluation of crystal-mixer performance in the superheterodyne receiver used. The crystal may be considered as network 1 and the spectrum analyser, that acts as an i-f amplifier here, as network 2.

Noise Temperature

It has already been noted that a crystal rectifier in general generates more noise than the Johnson noise produced by an equivalent resistor. The noise temperature t is defined as the ratio of the available noise power output of the crystal to that of a resistor at room temperature; that is

$$T = dN_0/kT_0df, \qquad (1\text{-}23)$$

where dN_0 is the available noise output of the crystal.

Relationships Between Noise Figures, Conversion Loss, and Noise Temperature

Eq. (1-4), substituted in Eq. (1-23), gives

$$t = FG, \tag{1-24}$$

whence, from Eq. (1-22)

$$F'_{rec} = L(t + F'_{i-f} - 1), \tag{1-25}$$

where the conversion loss L is the reciprocal of the conversion gain, F'_{rec} is the over-all effective noise figure of the crystal mixer and i-f amplifier, and F'_{i-f} is the effective noise figure of the i-f amplifier. From Eq. (1-25) it is seen that noise temperature and i-f amplifier noise figure are additive terms.

Optimum Operation of a Crystal Mixer

The conversion loss, noise temperature, and receiver noise figure are all functions of the balancing arm or the local oscillator power level. Fig. 22 shows the conversion loss and the noise temperature of a typical mixer type crystal as a function of rectified current. The noise-temperature curve is approximately linear over the range of interest. The conversion loss approaches a constant value as the rectified current is increased; above a rectified current of approximately 1 ma there is little change in conversion loss.

The effect of local-oscillator power level in an ordinary microwave receiver, or in the system under study, the effect of the reflectometer

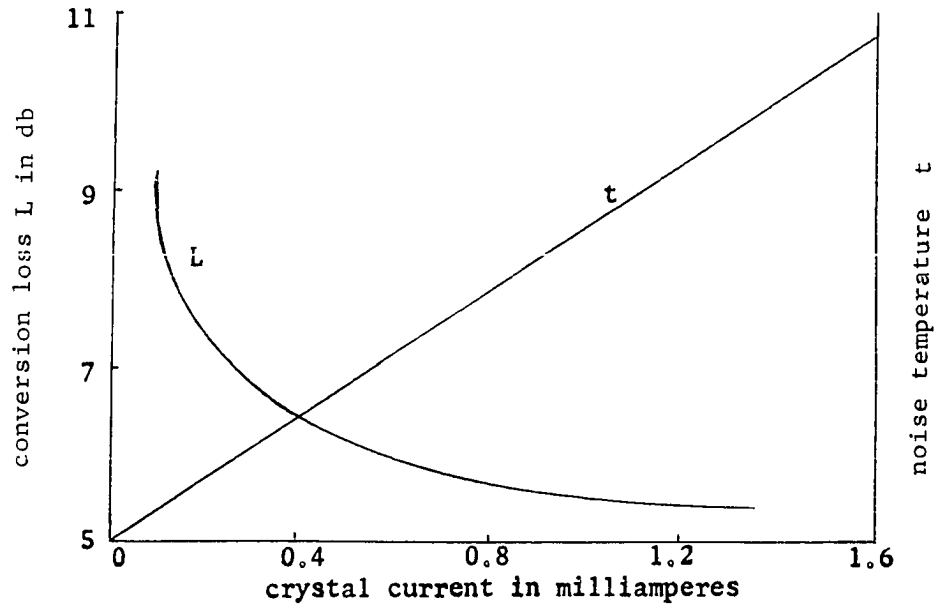

Fig. 22. Conversion loss L and noise temperature t as a function of rectified current for a typical 1N23B crystal rectifier.

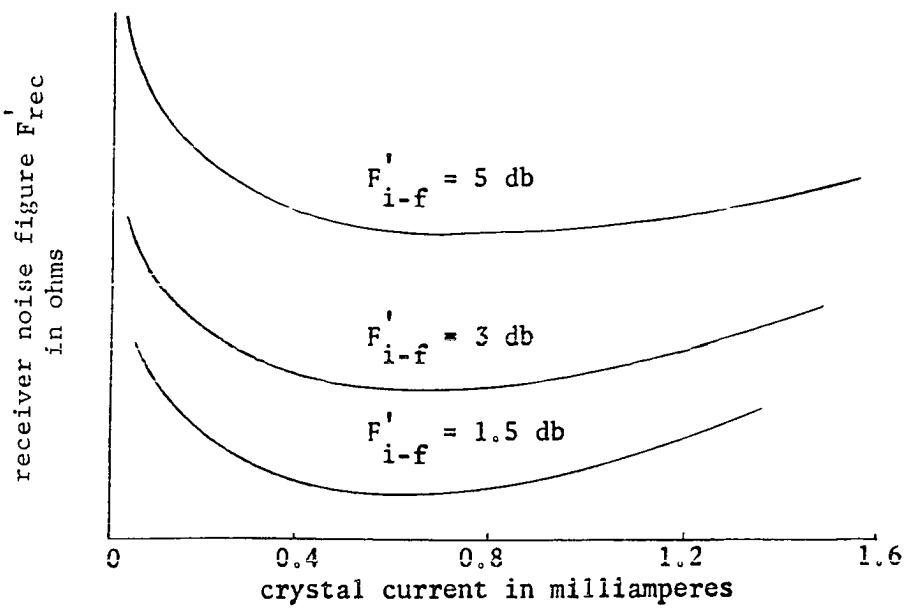

Fig. 23. Receiver noise figure F'_{rec} as a function of rectified current for a 1N23B rectifier plotted in Fig. 22.

balancing arm power level, on the noise figure can be obtained from the data of Fig. 22 by means of Eq. (1-25). The calculated curves for various values of i-f amplifier noise figure are as shown in Fig. 23. The curves are characterized in general by a broad minimum in the region of 0.3 to 0.8 ma and it is in this range that a crystal mixer must ordinarily operate for optimum performance. Since the minimum is broad, the choice of operating level is not critical. It is obvious from the curves that the minimum is broader for "quiet" crystals and would in fact disappear for a crystal having a noise temperature of unity for all values of rectified current. The shape of the conversion-loss curve makes it clear that even in this case there would be no point in operating at large values of rectified current. Indeed, as the curve suggests, it would be disadvantageous due to the presence of an appreciable amount of noise. The lower limit of operable range is obviously set by the rapid increase of conversion loss at low local oscillator power level.

Thus since the crystal used in the experiment was a mixer crystal 1N23B, a current of about 0.5 ma was maintained for optimum operation. Before observations were made on the microwave spectrum analyser, the output of the mixer was connected to a sensitive d-c meter. The power level of the balancing arm which is the local oscillator in the set up used here, is large compared with the level of the reflected wave so that the current read on the d-c meter is approximately equal to the so called local oscillator level. Therefore for maintaining the level for optimum operation adjustments were made on the attenuator at the imput arm of the Doppler reflectometer (H plane of the magic tee) and the balancing arm. The level of the reflected wave made very little difference for this specific adjustment.

APPENDIX 2

MICROWAVE REFLECTION FROM A PULSED DISCHARGE

Introduction

In an experimental study intended to determine the positive ion velocity in prebreakdown of a gas discharge [13,20], the values of the velocity obtained were in close agreement with the velocity of the slow striations obtained in prebreakdown [18]. This has already been discussed in Chapters III and IV.

This excellent experimental work was found in need of a theoretical study for quantitative verification. The work was then supplemented by the analysis, in this appendix, and the finding that the measurement made was in fact the slow striation velocity rather than ion velocity. From this important finding, the present program evolved in which the fast striations at the onset of ionization could be studied.

This analysis uses a generalization and application of a transient solution of Townsend discharge [19] to obtain the positive ion density under the conditions of the experiment performed. This density is then used to obtain the permitivity of the medium [30] from which the microwave reflection from the medium can be found using ordinary methods and making some appropriate simplifying assumptions on the boundary of the media.

The detailed solution of the analysis of the pulsed Townsend discharge, utilized here for determining the ion velocity, is avoided. Instead the method of analysis and the formulation of the problem, as well as the final solution which is applied to the present study, are given in sufficient detail. It was found necessary to go into the details of some of the manipulations [Eqs. (2-12) to (2-26)], the results of which appear in the final solution, in order to avoid complications involved in defining the quantities used in the solution.

The analysis will thus consist of two parts. First, the theoretical developments leading to a relation for the ion density ρ_i, which is the most complete analysis in which all the important secondary processes effective in the discharge, as well as their effect on the primary processes, are taken into account, but in which the striations are completely neglected. Second, a relation for the resulting reflection of the microwave signal at the boundary between the free space, from which the signal is impinged, and the ionized medium in the discharge tube.

Method of Analysis of a Pulsed Townsend Discharge Neglecting Striations

For this analysis it will be assumed that the discharge is between infinite parallel plates and that the cathode is irradiated so that an electron current i_0, called the primary current, is emitted. It is known that the steady state current through the discharge is given by [17]

$$i = i_0 \exp [\alpha_i(d-x_0)]/(1-\gamma\{ \exp [\alpha_i(d-x_0)] -1\}). \qquad (2\text{-}1)$$

Here, d is the separation of electrodes, and α_i, γ and x_0 are considered

to be functions of gas pressure and electric field. The first Townsend coefficient α_i is interpreted as the number of ionizing collisions which one electron makes while travelling one centimeter in the direction of the electric field x_0 is interpreted as the distance that an electron must travel before acquiring ionizing energy, and γ is interpreted as representing the number of electrons emitted from the cathode under the influence of various events which occur in discharge as will be discussed.

The fundamental picture of a gas discharge under consideration will be taken as follows: An electron which leaves the cathode encounters a certain number of gas molecules while travelling to the anode. If one of these collisions is inelastic, there may be three possible results: (1) the molecule may be ionized; (2) the molecule may be excited to a level from which it can decay by radiation; (3) the molecule may be excited to a metastable level. Subsequently, electrons may be emitted from the cathode (1) upon impact of a positive ion, (2) when radiation from an excited molecule strikes the cathode, and (3) when a metastable molecule strikes the cathode.

As will be seen later, this mechanism leads to an expression for γ in Eq. (2-1), which is the sum of three terms, one each from the electron emission caused by radiation, ions and metastables. The interest in the analysis of transient current, to be discussed here, lies among other things, in that it makes the separation of the above terms possible. Here, however, the purpose is to obtain for an unstriated discharge during prebreakdown a scattering theory of ionized gases, and thus find the reflection obtainable from a pulsed discharge, based on the denisty of the positive ions.

The basis for this analysis of the pulsed discharge lies in the different times required for radiation, ions, and metastables to produce effects at the

cathode. Suppose the discharge is initiated by an electron leaving the cathode. This electron and the ones released by ionization in the gas reach the anode at about the same time required for an excited molecule to radiate, and for the radiation to reach the cathode and produce a photoelectron. This time is of the order of 10^{-8} sec. An ion drifting under the field, does not reach the cathode for about 10^{-6} sec., while a metastable which must reach the cathode by diffusion, requires the order of 10^{-3} sec. Thus, transient should show three relatively distinct phases, governed by these differences in time required to produce new electrons at the cathode.

The first phase, of duration about 10^{-8} sec., in which the first electrons are crossing the tube and new photoelectrons are being produced, shall not be analysed for its form but it shall be shown how to allow for its effect upon other phases.

The form of the second phase characterized by the first arrival of positive ions at the cathode, will be obtained. It can be shown that, under certain conditions, it contains discontinuities in the current, which can be utilized for the observation of positive ion velocity [10,11].

The third phase is characterized by the first arrival of metastables at the cathode.

The analysis is performed by setting up boundary value problems to be satisfied by the densities of ions and metastables in the gas [19] and for any form of i_0 as a function of time, from which the ion density that results in the largest reflection of the electromagnetic wave incident on the discharge tube, can be found.

Amplification by Ionization and Radiation

It will be assumed that electrons cross the tube in negligible time. As a result of ionization in the gas, more electrons reach the anode than leave the cathode. If n_0 electrons leave one cm^2 of the cathode at some instant, it is well known that the number of electrons per cm^2 that reach a distance x from the cathode is given by

$$n = n_0 \exp \alpha_i (x-x_0), \qquad x \geq x_0, \tag{2-2}$$

For $x < x_0$, $n = n_0$.

Let α_r be the number of excited molecules created per electron per cm. The number of excited molecules per cm^2 created in a distance dx is $\alpha_r n dx$, if x is greater than x_r, the distance an electron must travel to acquire excitation energy. For brevity, the difference between x_0 and x_r will be neglected. Again if x is less that x_r, the number of excited molecules is zero.

Let Θ be the probability that a photon radiated at the distance x will reach the cathode. $\Theta = 2\pi$ if absorption in the gas is negligible. Let γ_r be the number of secondary electrons per photon. Then the number of secondary electrons is

$$\alpha_r \gamma_r n_0 \int_{x_0}^{d} (\Theta/4\pi) \exp [\alpha_i (x-x_0)] \, dx. \tag{2-3}$$

It will be assumed that these secondaries are emitted in negligible time, so that the effect of radiation is to increase the number of electrons leaving the cathode from n_0 to

$$n_0 \sum_{j=0}^{\infty} \{\alpha_r \gamma_r \int_{x_0}^{d} (\Theta/4\pi) \exp [\alpha_i (x-x_0)] \, dx\}^j$$

$$= n_0/\{1-\alpha_r \gamma_r \int_{x_0}^{d} (\Theta/4\pi) \exp [\alpha_i (x-x_0)] \, dx\}, \qquad (2-4)$$

when the geometric series converges [19]. Let the factor M_r by which n_0 is multiplied be called the multiplication factor for radiation.

Equation for the Ion and Metastable Density

Let $\rho_i(x,t)$ be the density of ions and $\rho_m(x,t)$ the density of metastables at time t at a distance x from the cathode. Also let the ions have a velocity v, so that the current of ions per cm^2 at any point is $-v\rho_i(x,t)$. It is further assumed that the metastables move by diffusion with a coefficient D, so that the current of metastables per cm^2 is $-D(\partial\rho_m/\partial x)$. Thus, the flow equations for ρ_i and ρ_m are:

$$\partial\rho_i/\partial t - \partial(v\rho_i)/\partial x = S_i(x,t), \qquad (2-5a)$$

$$\partial\rho_m/\partial t - \partial(D\partial\rho_m/\partial x)/\partial x = S_m(x,t), \qquad (2-5b)$$

where S_i and S_m are functions, now to be set up, which give the numbers of ions and metastables created per cm^3 per sec.

Let γ_i be the number of electrons liberated per positive ion striking the cathode, and γ_m the number of electrons per metastable. Then the total number of electrons leaving the cathode per cm^2 per second is

$$M_r [i_0 + \gamma_i v\rho_i(0,t) + \gamma_m D\rho_m'(0,t)], \qquad (2-6)$$

in which a prime denotes $\partial/\partial x$, and i_0 is the primary current density measured in electrons per cm^2 per sec. To get the number of electrons per cm^2 per sec. at a distance x from the cathode, i_0 will be multiplied by unity for $x<x_0$ and by $\exp[\alpha_i(x-x_0)]$ for $x \geq x_0$. If α_i is the number of ions formed per electron per cm, and α_m the number of metastables, Eqs. (2-5) become

$$\partial\rho_i/\partial t - v\partial\rho_i/\partial x = \alpha_i M_r(i_0 + \gamma_i v\rho_i(0,t) + \gamma_m D\rho_m'(0,t)]\exp[\alpha_i(x-x_0)], \qquad x \geq x_0 \tag{2-7}$$

$$\partial\rho_m/\partial t - D\partial^2\rho_m/\partial x^2 = \alpha_m M_r[i_0 + \gamma_i v\rho_i(0,t) + \gamma_m D\rho_m'(0,t)]\exp[\alpha_i(x-x_0)], \qquad x \geq x_0. \tag{2-8}$$

As auxiliary conditions to (2-7) and (2-8), the forms $\rho_i(x,t)$ and $\rho_m(x,t)$ must be known when $t=0$. These generally depend upon the type of transient being studied. In addition, there are certain conditions imposed upon ρ_i and ρ_m at the electrodes. For ρ_i, there is only one condition, which can be derived from the flow conditions at the anode:

$$\rho_i(d,t) = 0. \tag{2-9}$$

The conditions on ρ_m are more complicated. The boundary conditions are expected to be homogeneous in ρ_m and ρ_m', and hence of the form

$$\rho_m(0,t) - N_c d\rho_m'(0,t) = 0,$$
$$\rho_m(d,t) + N_a d\rho_m'(d,t) = 0, \qquad (2\text{-}10a)$$

which implies a relation between the density and the metastable molecular current at the boundaries. If both electrodes are of the same material, $N_c = N_a = N$. The sign is different in these two conditions because the normals to the two electrodes are oppositely directed. N can be shown [19] to have a value

$$N = (D/2d)(2\pi m/kT)^{1/2}(\gamma_m^{-1} - 1/2). \qquad (2\text{-}10b)$$

Using the kinetic theory expression for D [2], this is approximately

$$N = (4\lambda_m/3d)(\gamma_m^{-1} - 1/2), \qquad (2\text{-}11)$$

where λ_m is the mean free path of a metastable in an atmosphere of normal molecules. This has two important limiting cases; if $\gamma_m = 0$, N is infinite, and $\rho_m'(0,t)$ must vanish. If $\lambda_m/d \ll \gamma_m$, $\rho_m(0,t)$ very nearly vanishes.

Ion Transient and Steady State Currents

In the first several microseconds, ions can cross the tube a number of times before the metastables have moved appreciably. To study the operation of the tube during this interval, which is the main subject of this appendix, γ_m can be set equal to zero in Eq. (2-7). Also, a step function $\varepsilon(w)$ is defined by

$$\varepsilon(w) = \begin{cases} 1, & w \leq 0 \\ 0, & w > 0. \end{cases} \tag{2-12}$$

The use of this step function avoids some trouble with limits. Eq. (2-7) becomes

$$\partial\rho_i/\partial t - v(\partial\rho_i/\partial x) = \alpha_i M_r [i_0 + \gamma_i \rho_i(0,t)] \times \exp[\alpha_i(x-x_0)]\varepsilon(x-d)\varepsilon(x_0-x). \tag{2-13}$$

General Solution

For brevity, let

$$\phi(x) = \alpha_i M_r \exp[\alpha_i(x-x_0)]\varepsilon(x-d)\varepsilon(x_0-x). \tag{2-14}$$

Also transform the independent variables from x,t to t and $y = x+vt$, and let $\rho_i(x_i,t) = P_i(y,t)$. Then y is the coordinate which moves with the stream of ions. Eq. (2-13) will then become

$$\partial P_i/\partial t = [i_0 + \gamma_i v P_i(vt,t)]\phi(y-vt). \tag{2-13a}$$

Solutions of (2-13a) which have the proper form at $t=0$ are also solutions of the integral equation

$$P_i(y,t) = P_i(y,0) + \int_0^t \phi(y-vt')[i_0 + \gamma_i v P_i(vt',t')]dt' \tag{2-15}$$

The current can be calculated once the ion density is known. The current carried by positive ions is

$$i_+(t) = (v/d) \int_0^d \rho_i(x,t)dx$$

$$= (v/d) \int_{vt}^{vt+d} P_i(y,t)dy, \qquad (2\text{-}16a)$$

all in electronic charges per cm^2 per sec. The number of electrons leaving unit area of the cathode per sec. is

$$M_r[i_0 + \gamma_i v\rho_i(0,t)] = M_r[i_0 + \gamma_i vP_i(vt,t]. \qquad (2\text{-}17)$$

In addition to these electrons, there are those which are formed in the gas and which do not traverse the entire distance d. Since $\phi(x)/M_r$ is the number of new electrons created per cm per electron leaving the cathode, the total current carried by electrons will be obtained if the number of electrons leaving the cathode is multiplied by

$$M_g = 1 + \int_0^d [\phi(x)/M_r][(d - x)/d]dx. \qquad (2\text{-}18)$$

This weights each electron according to the distance it travels in reaching the anode. The current carried by electrons is therefore:

$$i_-(t) = M_r M_g[i_0 + \gamma_i vP_i(vt,t)]. \qquad (2\text{-}16b)$$

With the aid of this, (2-15) can be replaced by a similar equation.

Substituting from (2-16b) for the quantity in square brackets in (2-15), for $y = vt$, there is obtained:

$$P_i(vt,t) = P_i(vt,0) + \int_0^t \phi(vt-vt')[i_-(t')/M_r M_g]dt'. \qquad (2\text{-}19)$$

Substituting this back into (2-16b) results in

$$i_-(t) = M_r M_g[i_0 + \gamma_i v P_i(vt,0)] + \gamma_i v \int_0^t \phi(vt-vt') i_-(t')dt'. \qquad (2\text{-}20)$$

The desired function for this analysis is the positive ion density $\rho_i(x,t)$. Eq. (2-20) can be solved for $i_-(t)$, then $P_i(vt,t)$ can be computed from (2-16b) from which $\rho_i(x,t)$ can be obtained through the transformation of the independent variables. The solution will be continued as follows.

Eq. (2-20) is solved by Picard's method [9]. Let

$$i_-(t) = \sum_{n=0}^{\infty} i_-^{(n)}(t),$$

$$i_-^{(0)}(t) = M_r M_g [i_0 + \gamma_i v P_i(vt,0)], \qquad (2\text{-}21)$$

$$i_-^{(n+1)}(t) = \gamma_i v \int_0^t \phi(vt-vt') i_-^{(n)}(t')\, dt',$$

$$n = 0, 1, 2, \ldots$$

If the sum exists, it is the required solution.

Steady State Solution

Before applying (2-21), the steady-state solution is derived. This has significance, in the first place, if i_0 is constant and in the second place only if the ions can traverse the tube many times before metastables begin to reach the cathode in appreciable numbers. The first of these assumptions is necessary because of the initiation of ionization by natural sources using an overvolted gap is statistical and thus nonuniform. The second of these assumptions is reasonable on account of the motion of metastables through diffusion and as a result the smaller transit times involved for metastables. Under these circumstances, this steady state will be sensibly reached before the beginning of the metastable transient. For this reason, and because of the fact that for the present work only the time of transit of ions across the gap is of interest, metastable current will be neglected in the final analysis.

The steady state ion density $\rho_i(x,\infty)$ is found by setting $\partial/\partial t = 0$ in Eqs. (2-13) and integrating. The constant of integration is determined by the condition that $\rho_i(d,t) = 0$. The result is:

$$\rho_i = (i_0/v)[\int_x^d \phi(x')dx']/[1-\gamma_i \int_0^d \phi(x')dx']. \qquad (2\text{-}22)$$

The current can be found by applying Eqs. (2-16a) and (2-16b). If $\phi(x)$ is given by Eqs. (2-14), the current has the well-known form:

$$i_i = i_0 M_r \exp[\alpha_i (d-x_0)]/\{1 + \gamma_i M_r - \gamma_i M_r \exp[\alpha_i (dx-x_0)]\}. \qquad (2\text{-}23)$$

Pulse Transient

In order to consider a rectangular pulse, the result of a single pulse of stimulating current occuring at $t = 0$, will be superimposed on the steady-state solution. For the single pulse transient $i = 0$ for $t>0$. It will be assumed that n_0 primary electrons are released from the cathode in negligible time at $t = 0$ and that these are instantly increased to $M_r n_0$. Then:

$$P_i(y,0) = n_0\ \phi(y). \tag{2-24}$$

P_i and the current can now be found by substituting into Eqs. (2-21) and (2-28).

Returning to the original assumption about the form of $\phi(x)$, that is, to the form of Eq. (2-14) with a constant α_i, the following results are obtained:

$$\rho_i(x,t) = \alpha_i M_r n_0 \exp\ [A_i(\xi-\xi_0+\tau)]\Sigma[A_i M_r \gamma_i \exp\ (-A_i\xi_0)]^n \times I_n(\tau,\xi_0,\xi). \tag{2-25}$$

where $\tau = vt/d$, $\xi = x/d$, $\xi_0 = x_0/d$, all dimensionless quantities, and $A_i = {}_i d$. Also

$$I_n(\tau,\ \xi_0,\xi) = \int_{\tau+\xi-1}^{\min(\tau+\xi-\xi_0),\tau} I_{n-1}(\tau',\ \xi_0,\ 0)\ d\tau',$$

$$I_0(\tau,\ \xi_0,\xi) = \varepsilon(\xi+\tau-1)\varepsilon(\xi_0-\xi-\tau). \tag{2-26}$$

Solution of ρ_i for Maximum Reflection

Solution of Eqs. (2-7) and (2-8) subject to the boundary conditions previously discussed, is already found [19]. The form of this solution suitable for the intended analysis is

$$\rho_i = (i_0 d/v) M_r M_i \{\exp(\eta A_i) - \exp[A_i - (\xi - \xi_0)]\}, \quad \xi \geq \xi_0; \tag{2-27}$$

where ρ_i is in number of ions per cm^2 when the entire length of the tube is considered, $\eta = 1 - \xi_0$, and M_i is given by

$$M_i = \{1 + \gamma_i M_r - \gamma_i M_r \exp[\alpha_i (d - x_0)]\}^{-1}, \tag{2-28}$$

and where the other quantities are already defined. In computing ρ_i, such values of θ, i_0, α's and γ's will be chosen that will result in the largest value of ρ_i encountered.

Eq. (2-27), relating ρ_i to the measurable parameters of the discharge, can be used to obtain the reflection resulting when a microwave signal is impinged on the discharge with such an ion density. The method of analysis is outlined in the following section.

Reflection Coefficient of a Medium with Ion Density ρ_i

It is well known that when a wave propagates from one medium with an intrinsic impedance η_1 into another with intrinsic impedance η_2, the reflection coefficient R is given by

$$R = (\eta_2 - \eta_1)/(\eta_2 + \eta_1). \tag{2-29}$$

In this case one medium can be regarded as free space with $\eta_1 = (\mu_0/\epsilon_0)^{1/2}$ and the other the ionized medium inside the tube. The magnetic permeability of the ionized gas can be taken as equal to that of free space, namely μ_0. However, a macroscopic analysis of a medium with a distribution of charged particles ρ_i upon which an electromagnetic wave of frequency ω is impressed, results in a permitivity ϵ given by [30]

$$\epsilon = 1 - 4\pi\rho_i \, e^2/\epsilon_0 \, m\omega^2. \qquad (2\text{-}30)$$

Substituting the numerical value of ρ_i from Eq. (2-27) into (2-29), the reflection coefficient R will be obtained. From R, the fraction of the reflected wave can be found.

For the computation of ρ_i, the values of M_r and M_i must be calculated first from Eqs. (2-4) and (2-28). For these calculations such extreme values of Θ, α_i, α_r, γ_i, and γ_r are used [11,16,17] that will result the largest values of R so that the largest values of reflection possible are obtained. A value of $i_0 = 10^{-6}$ amp. amplitude and $\Theta = 2\pi$ are chosen for the computation. These result in the largest value of ρ_i. Similarly such values of α's and γ's are chosen [16,39] that will give maximum possible values of ρ_i. Under these circumstances a value of ρ_i of about 10^9 ions per cubic centimeter is obtained which will not result sufficient reflection to be observed. On the basis of Eqs. (2-29) and (2-30), a computation is made to find out the value of ρ_i necessary for a reflection coefficient $R = 0.1$ so that about 10 per cent of the incident power will be reflected. As a matter of fact, this does not take into account the power lost due to radiation and other effects since it assumes an infinite boundary layer, so

that $R = 0.1$ is a safe assumption to assure sufficient reflection. For such a reflection coefficient the required value of ρ_i is found to be of the order of 10^{14} ions per cubic centimeter.

It is thus seen that based on an analysis of the discharge that does not take into account the striation phenomena, no reflection of the microwave signal is possible. However, as mentioned in Chapter IV, the concentration of the ionized medium at a small fraction of the entire ionization tube may result in a much larger density in the ionized layers that are successively being produced according to Pekarek's theory discussed in detail in the context. It can thus be concluded that the observation originally intended to be the positive ion velocity is actually the velocity of the so called wave of stratification.

APPENDIX 3

FURTHER INVESTIGATION OF THE ORIGIN AND GROWTH OF STRIATIONS

General Considerations

It was discussed in Chapter IV that for further investigation along the lines of this work new experiments can be developed and further improvements made in the present techniques. For this purpose it was suggested that experimental investigations be made in which the ionization tube will be perturbed at different instants of time and different points along the tube and the resulting transients observed. To this end an impulse voltage can be used for the purpose of the perturbation which may be introduced at various points in the tube and at various times. In all cases care will have to be exercised to introduce the perturbation after the ionization has passed the point at which the perturbation is introduced. This is particularly important during the first crossing time of ionization.

The purpose of this appendix is to give further details of the proposed investigations, which are intended to reveal the phenomena related to the origin and the temporal growth of striations in gas discharges. These investigations must be performed in three distinct phases of the discharge. The first phase is from the start of the ionization until ionization progresses along the entire length of the discharge tube. It is in this phase that the

present results are obtained. The second phase is during the period before the glow of the ionized gas, which is referred to in the context of this work, as prebreakdown. It is distinct from the first phase in that it persists for a longer period of time. In the terminology used here, prebreakdown excludes the small period of the first phase. The third phase is during the glow phase of the discharge. In this phase there is no time limitation and the experiment can be carried out during as long a time period as necessary.

No data is available on the first phase except the data reported in this investigation. The only data available on the second phase is that performed by Neusel and Silver [18]. However, in both cases, there is need for controlled perturbations rather than relying on the perturbations caused by fluctuations occuring at random inside the tube. There is some data available on the third phase [3,26], but the only data of interest in this phase are those in which transient methods are used. In references 21, 22, and 26, the cathode end of the positive column is perturbed externally and the production of the resulting wave of stratification observed, as previously discussed. A rather different technique can be used for the study of the third phase. Besides, there is no reason to apply the perturbation only at the cathode end of the positive column because disturbances occuring in the discharge can occur at almost any point and it is only natural that for a study of their effects, the artificial ones also be applied at various points in the tube.

The experiment to be performed will essentially consist of introducing perturbations at different points in the tube for each of the three phases discussed above. However, fairly different techniques have to be used for introducing the perturbations for each phase of the ionization.

The first requirement for such experiments is a pulsed light source to start a uniform electron emission from the cathode. The reason for such a light source has already been discussed in detail in Chapter IV. It is a definite requirement for the proposed experiment. This is because by ionizing the tube in this manner the ionization can be controlled and the introduction of the pulse as well as the observation of the resulting transients can be carried out in synchronism with the light source or with a delay, whichever is necessary. The technique of synchronizing the perturbation of the observation of the resulting transients with a pulsed light source (and as a result with the initiation of the ionization) will be explained shortly. It is evident that such techniques will not be possible when ionization is initiated by statistical methods, as in the case when the overvoltage method is used.

In all three phases of ionization it is necessary that (a) the perturbation in the form of a voltage pulse be introduced after the ionization so that the voltage pulse must be triggered through a delay circuit by the light source, (b) the observation instrument, the oscilloscope or camera, also be triggered by the light source. The method of perturbation is similar for all three phases but it will be seen that for the observation of the results of the first phase, the technique used in the present investigation is advantageous over the other methods. For the other phases, a number of techniques are possible, namely the photo-tube and oscilloscope method, the rotating mirror photography, and the streak and frame photography.

At this point the major components to be used for the proposed investigations as well as the techniques for using them in the experiments will be discussed. An account of the basic design of the light source and its modification in order to fit the need of the experiments will be discussed

in detail. Other components in common use, such as the delay circuits and amplifiers will be shown in block diagram form.

Pulsed Light Source

For the short duration light source used for the improvement of the present technique, a conventional spark gap operating in air at atmospheric pressure energized by a pulsing circuit capable of supplying high current for a short time [1] can be used. Some modifications can then be made in order to make the spark gap suitable for use in the proposed set up. A brief description of this spark gap follows.

It is known that the spectral lines in an ordinary spark discharge due to gas appear first followed by the spark and are lines characteristic of the electrode material. The spectral lines of the gas are emitted with relatively high intensity during the high potential stage of the discharge before the low voltage arc is formed. That is, the first light emitted by the spark originates in the gas surrounding the electrodes. As the discharge progresses, vapor of the electrode material is formed on the electrodes and moves toward the center of the spark gap. This vapor gives rise to the spark and arc lines characteristic of the electrode material. At small gap spacings and minimum field strengths of transition from the high potential to the arc discharge takes place from 1 to 5×10^{-8} sec. This time is not to be confused with the lag of the spark, but refers to the time taken by the discharge when once started will continue to change from a high potential to a low potential type. This time can, of course, be made much longer by increasing the electrode separation using extremely non-uniform fields, etc., but for two electrodes with a reasonable field distribution and a gap spacing of one centimeter, it can be made less than 5×10^{-8} sec.

In the design of this light source, the current through the gap may be made to reduce to zero or to a very small value as soon as the arc type of discharge is formed and consequently limits the length of the current pulse to the high voltage transition period. After the removal of the external field there are, of course, various decay processes which prolong the emission. However, these are not serious for light flashes of 10^{-7} sec. duration or longer required for this work.

The transition period can be decreased and the light emission increased by overvolting the gap. It is known that the field strength in the gap in air at atmospheric pressure can be maintained at about 16 times the minimum value for periods up to 10^{-6} sec. without breakdown provided the gas surrounding the electrodes is free from dust nuclei, ion, etc. [16]. If during this period of high field the discharge is initiated by the liberation of an electron at the cathode surface, the light intensity should be greatly increased and the transition period decreased. While this gap would seem to have decided advantages, the design can be carried out without using it to avoid high voltages.

The circuit to be used is shown in Fig. 24. It consists of a transmission line, open ended at the output, and shunted at the input end by a spark gap in series with a resistance equal to a surge impedance of the line. The line is charged initially from a conventional rectifier circuit with the charging current limited by high resistances to a few milliamperes. For random flashes, the line is charged slowly until the spark gap discharges.

The operation of the circuit is simple in principle. When the spark gap breaks down a discharge wave travels from the input end, is reflected at the output end, and returns to the input end reducing the potential of the

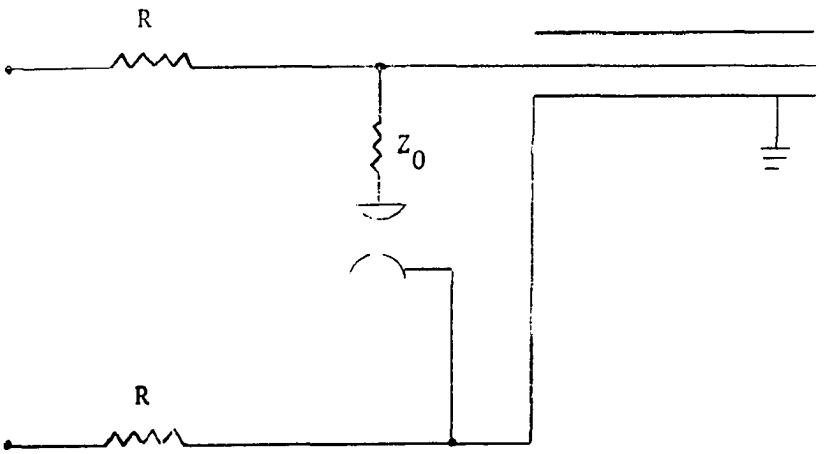

R = discharge resistance

Z_0 = resistance equal to surge impedance of the line

Fig. 24. Circuit diagram for the pulsed light source.

line to zero. This of course implies that the spark gap resistance has decreased to a value low compared with the characteristic impedance of the line by the time the reflected wave returns to the input end. If this is not the case, there will be reflection at the input end and the discharge will be prolonged. This means that the time length of the line should be at least as long as the transition period of the discharge. To increase the intensity

of the light two or more transmission lines can be connected separately to the gap electrodes through a resistance equal to its characteristic impedance. It is extremely important to keep the length of the connecting wires at an absolute minimum and to use non-inductive resistors in the discharging circuit. A conventional type gap can be used with the discharge viewed in the axial direction through a small hole in one electrode.

A modified form of the above light source can be used as shown in Fig. 25. The principal changes consist in (1) replacing the distributed

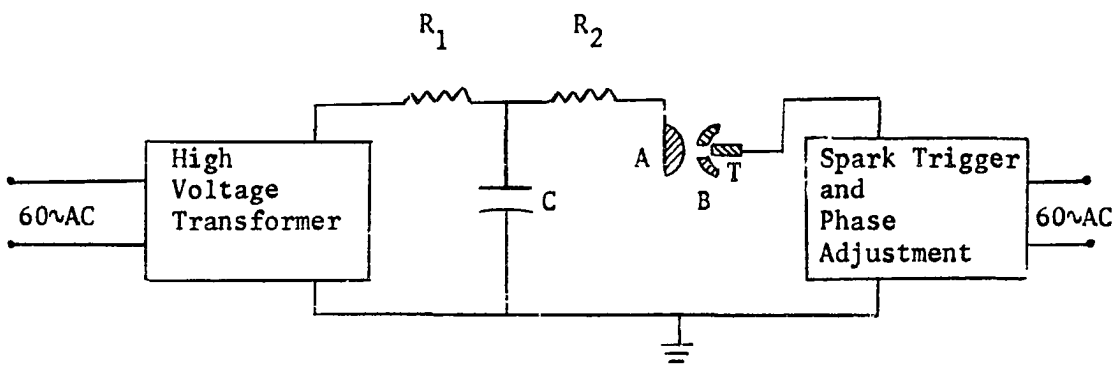

Fig. 25. Schematic diagram of pulsed light source. A and B are main electrodes, T is the trigger electrode (Reference [10]: permission requested).

capacitance transmission line by a small lumped capacity, (2) triggering the source regularly at a fairly low repetition rate so that the tube will completely extinguish after a pulse disappears before the next pulse is applied. The easiest rate to choose is 60 Hz. The triggering is thus easily accomplished by using an a-c transformer as the high voltage supply and arranging for the trigger voltage to be applied in the proper time phase. This gives a short light pulse which is intense, with appreciable energy in the ultra-violet.

The Experimental Apparatus

A conbination block diagram - schematic of the proposed experimental set up is shown in Fig. 26. All operations are triggered from the spark light source, which can operate at a repetition rate of 60 Hz.

Light in pulses is focused by a quartz lens system and passes through a quartz window (not shown) on to the cathode. The potential difference across the electrodes can be established by a continuously variable d-c power supply with a variable resistor in series with it to limit the current for experiments in the glow phase. In order to synchronize, or delay, the time of the introduction of the pulse of perturbation, or the time of observation of the light intensity after the perturbation, with the time of initiation of ionization. Part of the incident photopulse can be reflected by a partial mirror into a vacuum phototube. In this way a current is developed which is in phase with the light pulse and thus with the onset of ionization in the tube. This current can then be used for delay circuits which will trigger both the pulse of perturbation and the instrument on which the outcome of the perturbation is to be observed. This instrument

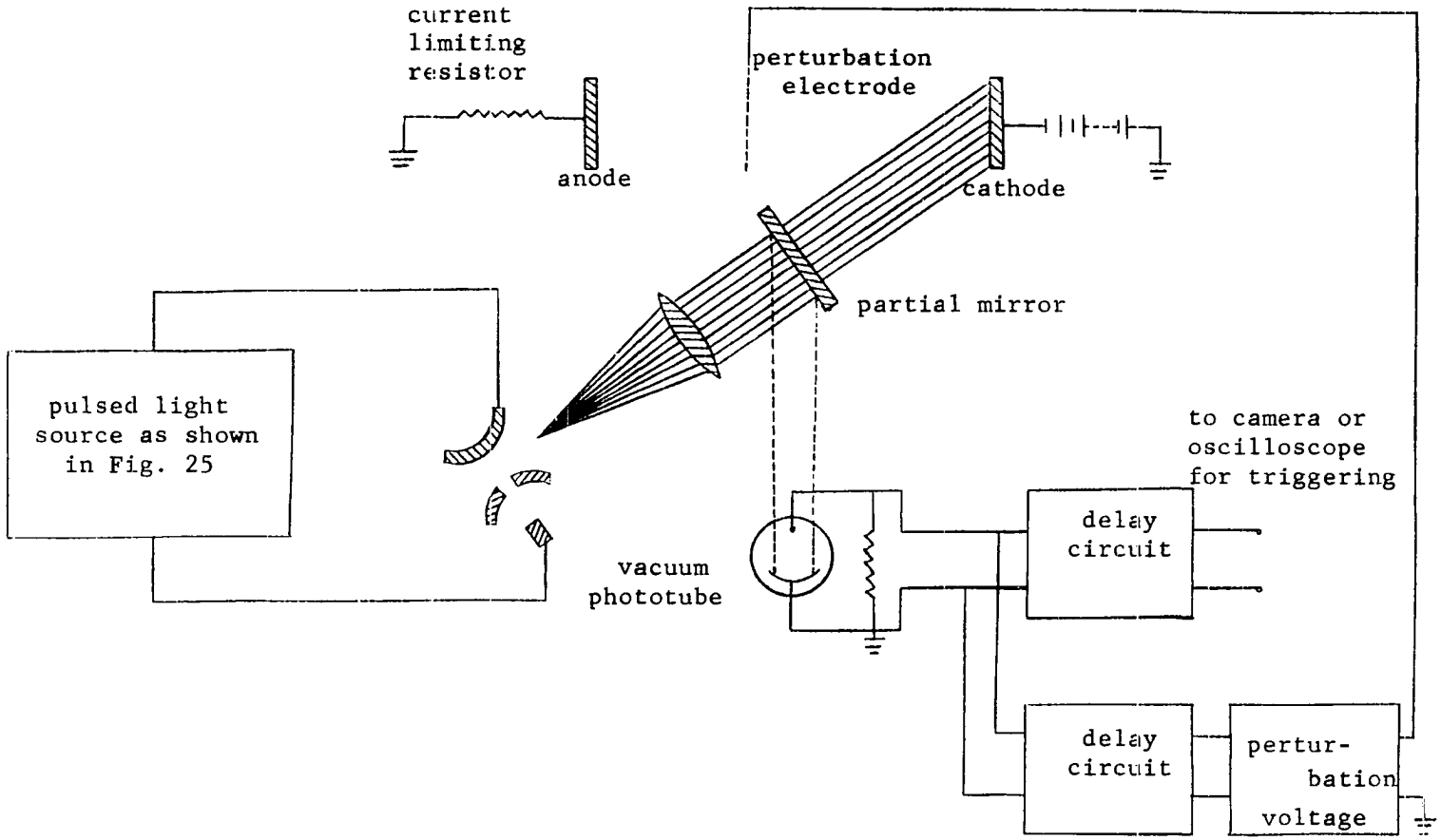

Fig. 26. Block diagram-schematic representation of experiments for investigating striations.

may be a camera as used by Neusel and Silver [18] or phototubes and oscilloscope as used by Donahue and Dieke [3] and later by Pekarek [21]. The most suitable method for the observation of the first phase of ionization is the one used in the present investigation because the light intensity is weak. In this case then the triggering of the observation instrument is not necessary.

It is important that the tube be perturbed at different points for all phases of ionization. According to conventional theories on ionization growth which do not take into account the phenomena leading to striations, similar processes occur throughout the period of prebreakdown. It can thus be conceived that the phenomena of the nature described here occur all along in prebreakdown. Thus, the introduction of an external perturbation is equivalent to magnifying these random phenomena, which take the form of perturbations, and thus observe more vividly and in a controlled manner, the effect of such perturbations. It is thus reasonable to expect that such random phenomena can occur at various points in the tube and it is therefore necessary to apply the artificial perturbations at different points along the tube.

For the case of a glow discharge, however, it is known that different processes lead to the existence of various dark and glow regions. These regions are predicted for a steady state glow, based on analyses that neglect the phenomena leading to striations [39]. Such analyses thus lead to the existence of an unstriated positive column. Disturbances in the positive column and elsewhere in the tube may cause the existence of striations. It is therefore essential that the perturbations be introduced at different points in the glow discharge. The result of such perturbations, as well as

those in the prebreakdown right from the beginning of the ionization, may reveal some facts on the origin and temporal growth of ionization. This is the purpose of the experiments proposed in this appendix. No such experiments are known to have been performed.